https://doi.org/10.5194/egusphere-2026-3334
Preprint. Discussion started: 22 June 2026

Deep-water hydrographic variability in the Northeast Atlantic during MIS 4

Svetlana Radionovskaya[1], Mervyn Greaves[1], David J. R. Thornalley[2], Luke C. Skinner[1]

[1]Department of Earth Sciences, University of Cambridge, Cambridge, CB2 3EQ, UK
[2]Department of Geography, University College London, London, WC1E 6BT, UK

Correspondence to: Svetlana Radionovskaya (sr632@cam.ac.uk)

Abstract. Understanding the evolution of deep ocean circulation and chemistry over the last glacial cycle is key for elucidating the ocean's role in modulating atmospheric CO_2 changes on millennial and orbital timescales. Marine Isotope Stage (MIS) 4 is a key paleoclimatic interval of the last glacial inception for assessing the role of the deep-ocean carbon storage in driving atmospheric CO_2 levels, because it is characterized by a large decrease of air temperature and a rapid atmospheric CO_2 drop of ~40 ppmv, likely linked to changes in ocean circulation, and includes several millennial climatic events, for example Heinrich Stadial (HS) 6. Although previous proxy-based studies have suggested a weakened Atlantic overturning during MIS 4, and particularly HS 6, basin wide changes in circulation remain poorly constrained. Here, we present high-resolution deep-water hydrography reconstructions from the mid-depth Iberian Margin (core MD01-2444, ~2.65 km water depth), based on benthic foraminiferal Mg/Ca-derived deep-water temperature (T_{dw}), benthic $\delta^{18}O$, and associated $\delta^{18}O_{dw}$ records, alongside $\overline{SS}$- based flow-speed record. Our data reveal three distinct deep-water hydrographic 'regimes' at the Iberian Margin: 1) warm "interglacial-like" mode during MIS 5a (including Greenland stadials C19 and C20); 2) a colder glacial circulation mode during early MIS 4 (pre- HS 6); and 3) a "Heinrich" circulation mode during HS 6. A stronger influence of colder southern-sourced waters is inferred at the Iberian Margin throughout MIS 4 and intensifies during HS 6, whereas MIS 5a stadials are characterised by a pronounced subsurface warming. The warm stadials C19 and C20 were likely driven by a southward displacement of convection sites in the North Atlantic and appear to be unique to MIS 5a as they are not observed during MIS 3 Dansgaard-Oeschger events at this site. We also find evidence of "millennial-type" variability and, similar to recent studies for MIS 2, a persistent contribution of northern sourced waters during MIS 4 (pre- HS 6). The contrasting impacts of similar millennial-scale DO-type variability on North Atlantic deep-water hydrography and circulation strength during MIS 3, 4, and 5 highlight the strong dependence on the background climate state.

1 Introduction

Ocean circulation played a key role in controlling and modulating climatic changes over the last glacial cycle through its impacts on both heat transport and the carbon cycle. Thus, understanding the evolution of deep ocean circulation and

https://doi.org/10.5194/egusphere-2026-3334
Preprint. Discussion started: 22 June 2026

chemistry over the last glacial cycle is important for elucidating the ocean's role in driving atmospheric CO_2 changes on millennial and orbital timescales (e.g. Galbraith and Skinner, 2020; Sigman and Boyle, 2000). However, the spatial and volumetric extent, and the transport rate of North Atlantic Deep Water (NADW) remain ambiguous in both proxies and models, especially beyond the Last Glacial Maximum (LGM), leaving possible impacts on CO_2 changes elusive.

Ocean circulation during the LGM has been extensively studied. Using various proxies, such as benthic $\delta^{13}C$, εNd and radiocarbon, it has been suggested that NADW shoaled and consequently the southern sourced waters (SSW) dominated the Atlantic Ocean volume below ~2 km (e.g. Curry and Oppo, 2005; Lippold et al., 2016; Pöppelmeier et al., 2023; Skinner et al., 2017). However, recent studies have challenged these findings (Blaser et al., 2025; Howe et al., 2016; Pöppelmeier et al., 2020; Skinner et al., 2021; Wharton et al., 2026). The strength of Atlantic Meridional Ocean Circulation (AMOC) during the LGM (i.e. transport rate) is also debated. Some $^{231}Pa/^{230}Th$-based reconstructions imply a weaker glacial AMOC (Böhm et al., 2015; Lippold et al., 2016; Mcmanus et al., 2004), whilst others have found a stronger LGM southward transport in the mid-depth Northeast (NE) Atlantic and weaker in the Northwest (NW) Atlantic (Gherardi et al., 2005; Ng et al., 2018). Paleoclimate Modelling Intercomparison Project (PMIP) numerical models under glacial boundary conditions of varying generations show no agreement on either the geometry or the strength of the LGM AMOC (Kageyama et al., 2021; Muglia and Schmittner, 2015; Otto-Bliesner et al., 2007), with the most recent PMIP 4 ensembles showing a strong LGM AMOC (Kageyama et al., 2021) alongside other modelling studies (Galbraith and De Lavergne, 2019; Klockmann et al., 2016; Sherriff-Tadano et al., 2018). However, many other modelling LGM simulations corroborate reduced NADW extent (and transport strength) (e.g. Galbraith and De Lavergne, 2019; Menviel et al., 2017; Menviel et al., 2020).

Previous proxy studies have inferred, largely from sedimentary $^{231}Pa/^{230}Th$ data, that Heinrich events, and especially HS 1, are associated with a near cessation, or severe reduction of NADW leading to decreased bottom-water ventilation in the North Atlantic (e.g. Böhm et al., 2015; Bradtmiller et al., 2014; Henry et al., 2016; Mcmanus et al., 2004; Ng et al., 2018), although the robustness of this proxy to AMOC has been questioned (e.g. Leal et al., 2025; Lerner et al., 2020). Similarly, numerical model freshwater hosing simulations of Heinrich events lead to "AMOC shutdown" (i.e. the weakening and shoaling of NADW) under glacial and preindustrial boundary conditions (e.g. Ganopolski and Rahmstorf, 2001; Gottschalk et al., 2019; Kageyama et al., 2013; Menviel et al., 2008), although the results of these models may be biased due to their low spatial resolution impacting freshwater distribution and being forced with unrealistic freshwater volumes. More realistic forcing yields much more muted changes (Ivanovic et al., 2018) more consistent with recent integrated proxy data-model simulations (Pöppelmeier et al., 2023).

During glacial MIS 4, proxy records of circulation and/ or hydrography are more scarce than for the LGM, and no modelling experiments have been performed to date to assess the state of AMOC under MIS 4 boundary conditions, notwithstanding broader climate model simulations of MIS 4 using intermediate complexity models (e.g. Brovkin et al., 2012; Timmermann

https://doi.org/10.5194/egusphere-2026-3334
Preprint. Discussion started: 22 June 2026

et al., 2010). Yet, MIS 4 is a critical paleoclimatic interval of the last glacial inception, characterised by severe and sustained cold conditions in both hemispheres (e.g. Jouzel et al., 2007) and a rapid atmospheric CO_2 drop of ~40 ppmv (Bereiter et al., 2012). Sea level was significantly lowered during MIS 4, albeit not as low as during the LGM (e.g. Gowan et al., 2021; Rohling et al., 2017), implying that Laurentide Ice Sheet alongside other northern hemisphere ice sheets were most extensive during the LGM (Batchelor et al., 2019; Gowan et al., 2021; Toucanne et al., 2023). However, globally more extensive glaciers are thought to have been present during MIS 4 as compared to the LGM (Doughty et al., 2021; Hughes et al., 2013). MIS 4 includes several millennial climatic events including HS 6 at the end of MIS 4, which was comparable in climatic severity to HS 1 (e.g. Davtian and Bard, 2023; Hoogakker et al., 2015).

Several studies have suggested a change in AMOC during the MIS 5a/ 4 transition using: εNd records from the Indian and South Atlantic Oceans (Piotrowski et al., 2009; Piotrowski et al., 2005); $^{231}Pa/^{230}Th$ records from the NW Atlantic (Böhm et al., 2015) and NE Atlantic (Guihou et al., 2010); sortable silt records from the NW and NE Atlantic (Hall and Mccave, 2000; Thornalley et al., 2013); benthic B/Ca records (Yu et al., 2016) and benthic $\delta^{13}C$ (Govin et al., 2009; Martrat et al., 2007; Oliver et al., 2010; Piotrowski et al., 2005; Thornalley et al., 2013). Whilst all the available records agree that the transport was likely reduced and NADW shoaled during HS 6, the circulation mode during early MIS 4 (pre-HS 6) is unclear, with proxy records providing either muted, poorly resolved, or conflicting results. Other studies have used indirect proxy evidence to infer a mode change in AMOC during MIS 5a/ 4 transition, implying a shift from NADW to southern-sourced deep-water dominance (Barker and Diz, 2014; Bereiter et al., 2012; Hoogakker et al., 2015).

Additionally, MIS 5a stadials C19 and C20 may represent a circulation state distinct from that of MIS 4 and HS 6 (e.g. Böhm et al., 2015; Thornalley et al., 2013). These millennial-scale climatic events occur under relatively "interglacial" background conditions of MIS 5a, yet are characterised by extremely cold conditions in Greenland as inferred from Greenland ice core records (Ngrip Project Members, 2004). In particular, C19 appears to have been as cold as glacial conditions of MIS 4 and the LGM. In contrast, North Atlantic % *N. pachyderma* -based sea surface temperature records indicate that substantial cooling did not occur until the MIS 5a/ 4 transition with only muted, if any, increase in *N. pachyderma* during C19 and C20 stadial events (e.g. Barker et al., 2015; Bauch et al., 2012; Mcmanus et al., 1994; Thornalley et al., 2013; Voelker and De Abreu, 2011; Zeng et al., 2025; Zeng et al., 2023), thereby supporting the persistence of relatively "interglacial" climatic state. High resolution reconstructions of North Atlantic circulation are therefore needed to assess changes before, during, and after the MIS 4 glacial interval.

One way to assess changes in deep-water hydrography, and by extension circulation, is by reconstructing deep-water temperature (T_{dw}) and local associated $\delta^{18}O_{dw}$ change (e.g. Mawbey et al., 2026; Roberts et al., 2016; Skinner et al., 2007; Skinner and Elderfield, 2007; Skinner et al., 2003; Wharton et al., 2026). However, existing benthic Mg/Ca-based T_{dw} records spanning part or all of the ~55-85 ka interval (El Bani Altuna et al., 2021; Elderfield et al., 2012; Ezat et al., 2014;

https://doi.org/10.5194/egusphere-2026-3334
Preprint. Discussion started: 22 June 2026

Marcott et al., 2011; Thomas et al., 2025) lack the temporal resolution necessary to resolve the key millennial- and/ or orbital-scale events that occurred during this period.

Here we present ~55-85 ka interval high-resolution benthic foraminiferal Mg/Ca- based T_{dw} reconstructions, benthic $\delta^{18}O$, and associated $\delta^{18}O_{dw}$ records from the mid-depth Northeast Atlantic (Iberian Margin) sediment core MD01-2444 (~2.65 km water depth) to investigate changes in deep-water hydrography, alongside sortable silt ($\overline{SS}$)- based flow speed record. Whilst this site is influenced by Northeast Atlantic Deep Water (ENADW) today, numerous studies have shown that during past glacial climatic stages, contribution of southern-sourced water was likely more significant in the mid-depth Northeast Atlantic, and at the location of site MD01-2444 (e.g. Hodell et al., 2023; Martrat et al., 2007; Skinner et al., 2007; Skinner et al., 2003). Thus, this site is well suited to investigate changes in past NADW and AMOC dynamics.

2 Study Area

Today, study site MD01-2444 (37°33.88' N, 10°08.34' W, 2656 m) is bathed primarily by Northeast Atlantic Deep Water (ENADW) (Hodell et al., 2023; Hodell et al., 2014; Van Aken, 2000), a water mass characterised by low temperature and salinity (with respect to surface water masses) and high oxygen content (Liu and Tanhua, 2021), occupying ~1.5-4 km water depths. ENADW is in turn made up of several water masses: the eastern branch of (Classical) Labrador Sea Water (LSW) (also known as Upper North Atlantic Deep Water, UNADW) found at depths ~1.5-2.2 km with the main core located at ~1.8 km, Iceland-Scotland Overflow Water (ISOW) occupying depths ~2.2-4 km (Garcia-Ibanez et al., 2015; Liu and Tanhua, 2021; Van Aken, 2000) and Lower Deep Water (LDW) (Van Aken, 2000). ENADW at the Iberian Margin is primarily made up of ~45% LSW (Jenkins et al., 2015; Thomas et al., 2022), ~10% ISOW (Garcia-Ibanez et al., 2015; Thomas et al., 2022) and ~45% LDW (Van Aken, 2000).

At abyssal depths, >4km, LDW is found, characterised by low salinity (with respect to surface water masses), temperature, and dissolved oxygen concentration, and high nutrient content (particularly silica) (Garcia-Ibanez et al., 2015; Liu and Tanhua, 2021; Van Aken, 2000). Meanwhile, intermediate depths at the Iberian Margin, overlaying ENADW, are dominated by Mediterranean Outflow Water (MOW), characterised by warm temperatures, high salinity and low oxygen concentration (Guo et al., 2020; Van Aken, 2000). Shipboard CTD measurements from Iberian Margin cruise JC089 show that MOW has no influence below 2 km depth and that its core is located between ~500-1500 m (Hodell et al., 2014).

https://doi.org/10.5194/egusphere-2026-3334
Preprint. Discussion started: 22 June 2026

3 Methods

3.1 Chronologies

Several age models have been previously published for site MD01-2444. However, most either do not span MIS 4 (e.g. Margari et al., 2020; Vautravers and Shackleton, 2006) or are not detailed enough, whereby some of the millennial events are misaligned during MIS 4 (Hodell et al., 2013; Hodell et al., 2023). Thus, we created a new age model for site MD01-2444, reported in Radionovskaya and Skinner (in review). Briefly, MD01-2444 planktic (*G. bulloides)* $\delta^{18}O$ record was stratigraphically aligned to the abrupt millennial events in the NGRIP $\delta^{18}O$ ice core record (Ngrip Project Members, 2004), following previous studies (Margari et al., 2020; Shackleton et al., 2000; Vautravers and Shackleton, 2006). Tie-points were selected at the mid-points of each rapid millennial transition. Assuming uniform age uncertainties of 300 years for each stratigraphic alignment tie point date (assumed to reflect two standard deviations; the dating uncertainties in the ice core chronologies and the correlation uncertainties), a Bayesian age model was created using the Bchron statistical software package (Haslett and Parnell, 2008; Parnell et al., 2008) and running the MCMC algorithm for 10,000 iterations. The resulting mean (absolute) age uncertainty is ~1000±400 years, although these uncertainties are likely overestimates as Bchron arguably provides a maximal estimate of uncertainty (Trachsel and Telford, 2017). All records are reported on GICC05 (Rasmussen et al., 2006) and GICC05modelext timescales (Seierstad et al., 2014; Wolff et al., 2010), unless stated otherwise. New tie points for site MD01-2444 are shown in Fig. 1c versus NGRIP $\delta^{18}O$ and *G. bulloides* $\delta^{18}O$.

The $\overline{SS}$ record from site MD01-2444 (this study) is compared to the published $\overline{SS}$ records of Thornalley et al. (2013) from Northwest Atlantic sites ODP-1055 and ODP-1057. The age models of these sites were updated to allow comparison between the two records, because the original age models were aligned to the GICC05 timescale for 0-60ka interval only and a speleothem-tuned age model was provided prior to 60ka. Using previously published planktic $\delta^{18}O$ (*G. ruber)* from site ODP-1055 (Thornalley et al., 2013) and ODP-1057 (Evans et al., 2007), revised GICC05-based stratigraphic tie points were established for MIS 5a, consistent with tie points used for site MD01-2444 (table 1, Fig. 1a,b). The original age model from Thornalley et al. (2013) was used for depths <12.86 cm and <10.76 cm for sites ODP-1055 and ODP-1057, respectively.

https://doi.org/10.5194/egusphere-2026-3334
Preprint. Discussion started: 22 June 2026

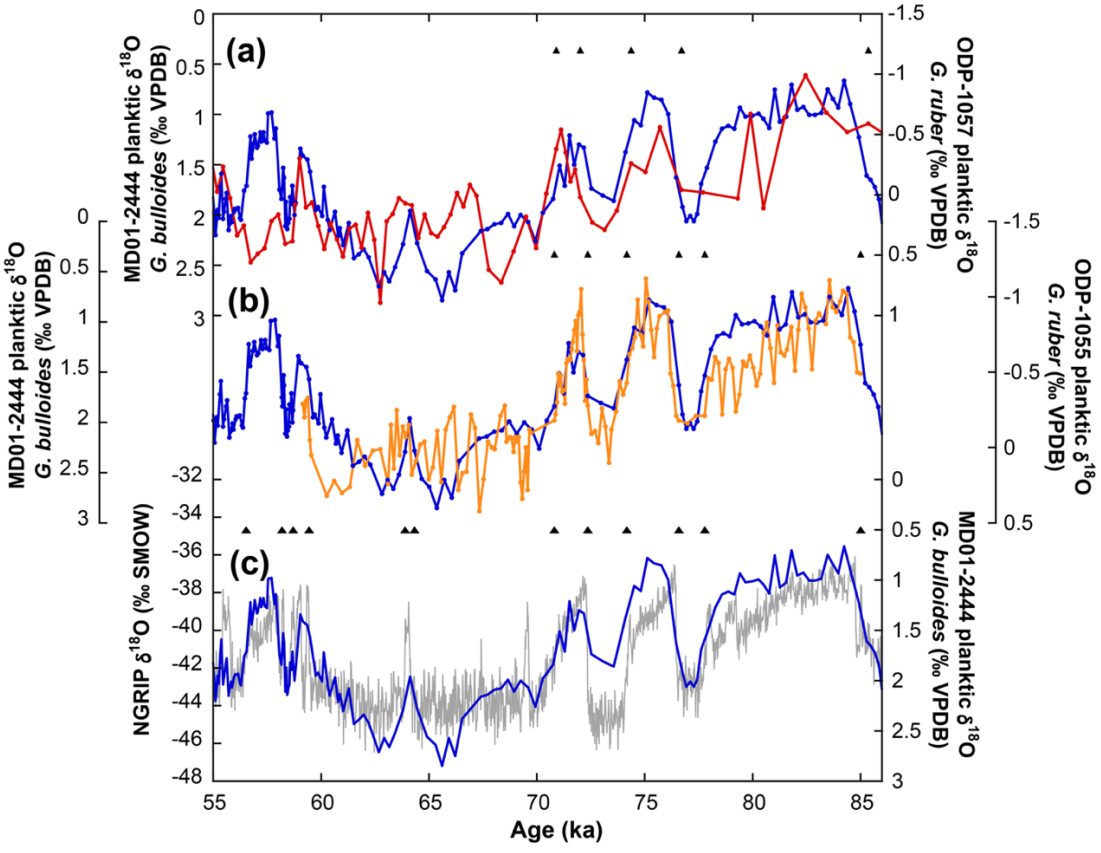

150 **Figure 1. Age models for sediment cores (a) ODP-1057, (b) ODP-1055 and (c) MD01-2444, with new tie points shown using black triangles. MD01-2444 planktic (*G. bulloides*) $\delta^{18}O$ (blue, this study) is shown versus: a) ODP-1057 planktic (*G. ruber*) $\delta^{18}O$ (red, (Evans et al., 2007; Thornalley et al., 2013)); (b) ODP-1055 planktic (*G. ruber*) $\delta^{18}O$ (orange, (Thornalley et al., 2013); (c) NGRIP $\delta^{18}O$ (grey, (Ngrip Project Members, 2004).**

Table 1: New updated age-depth tie points for site ODP-1055 and ODP-1057.

Depth ODP-1055 (MCD)	Age (ka) on GICC05 extended timescale	Depth ODP-1057 (MCD)	Age (ka) on GICC05 extended timescale
12.84	70.8	10.78	70.9
13.59	72.36	11.03	72
13.92	74.16	11.23	74.37
14.49	76.58	11.38	76.7
14.58	77.78		
14.93	85	11.88	85.36

https://doi.org/10.5194/egusphere-2026-3334
Preprint. Discussion started: 22 June 2026

3.2 Samples and materials

Core MD01-2444 (37º33.88' N, 10º08.34' W, 2656 m) was retrieved from the southwestern Iberian Margin during the 2001 R/V *Marion Dufrense II* Geosciences Cruise at a water depth of 2656 m using a Calypso giant piston corer (e.g. Hodell et al., 2013; Vautravers and Shackleton, 2006). Core MD01-2444 is ~27 m long and spans the last ~194 ka to MIS 7 with a mean sedimentation rate of 14 cm ka^{-1} (Hodell et al., 2013).

3.3 Stable Isotopes

Between ~7-50 specimens of deep infaunal *G. affinis* were picked from the >212 μm size fraction at 3 cm intervals between depths 1384-1647 cm. The samples were gently crushed between two glass plates to open all the chambers, homogenised and split into two aliquots. The smaller batch was used for stable isotope analysis, whilst the remainder was used for trace metal analysis (section 3.4), where sufficient *G. affinis* material was available. The weight used for stable isotope analysis was ~100-200 μg.

Stable isotope measurements were performed on a Micromass Multicarb Sample Preparation System attached to VG SIRA Mass Spectrometer, at the Godwin Laboratory for Paleoclimate Research, Department of Earth Sciences, University of Cambridge, following previously described methods (Hodell et al., 2015). All stable isotope measurements were calibrated to VPDB (Vienna Pee Dee Belemnite) international standard via international standards NBS19 and IAEA-6603 and internal Carrrara marble and Atlantic II standards. Long-term instrument analytical precision was better than ±0.08‰ for $\delta^{18}O$ and ±0.06‰ for $\delta^{13}C$. *Cibicidoides wuellerstrorfi* $\delta^{18}O$ and $\delta^{13}C$ have been previously reported by Hodell et al. (2023).

3.4 Trace metal analysis

G. affinis picked samples were divided into aliquots for stable isotope and trace metal analysis (section 3.3). The starting weight used for trace metal analysis was between ~150-700 μg, with most samples >300 μg.

All samples were subjected to the same standard foraminiferal chemical cleaning protocol following Barker et al. (2003). Briefly, the cleaning protocol involved: 1) clay removal using Milli-Q de-ionised water, methanol and seven to ten ultrasonication repetitions (note, that 7-10 ultrasonication repetitions were performed opposed to the five repetitions suggested by Barker et al. (2003)); 2) oxidative cleaning to remove organic matter adding 0.1M NaOH buffered 1% H_2O_2, heating up to ~90-100ºC for 10 minutes with subsequent rinsing, repeated twice; 3) mechanical removal of coarse-grained silicates (and any other visible discoloured particles and unopened foraminiferal chambers) using a fine brush, subsequently transferring each sample into a clean micro-centrifuge tube; 4) a dilute acid leach by adding 250 μl of 0.001M HNO_3 to each sample, followed by ultrasonification and rinsing.

https://doi.org/10.5194/egusphere-2026-3334
Preprint. Discussion started: 22 June 2026

All cleaned samples were dissolved in 0.1M nitric acid, diluted and analysed on an Agilent 5100 ICP-OES at the Department of Earth Sciences, University of Cambridge, to establish [Ca] following De Villiers et al. (2002) and using the standards from Greaves et al. (2005). All samples were subsequently re-diluted to 100ppm [Ca] and the trace element concentrations were analysed on an Agilent 5100 ICP-OES. The short-term instrument precision for Mg/Ca measurements, analysed using in-house solution R4 consistency standard (Mg/Ca within "standard" foraminiferal range) yielded analytical uncertainty of ±0.041 mmol/mol and precision of 0.79% r.s.d. for all runs.

3.5 Trace metal data contamination assessment

Contamination of the foraminiferal Mg/Ca signal may arise from two sources. First, clay contamination by alumno-silicate minerals, which contain 1-10% Mg by weight (Barker et al., 2003). An incomplete removal of clay from foraminiferal samples during cleaning (i.e. inefficient cleaning) will bias the final Mg/Ca ratios obtained. Second, the presence of authigenic (post-depositional) ferromanganese (Mn carbonate or Fe-Mn oxyhydroxide) carbonate coating, which contains a high amount of Fe and Mn (and some Mg) will bias the Mg/Ca signal, if present (Barker et al., 2003). The addition of reductive cleaning step using hydrous hydrazine into the foraminiferal sample cleaning protocol may be used to remove the authigenic coating (Boyle and Keigwin, 1985). However, such a step also leads to preferential dissolution of Mg-rich foraminifer calcite leading to lower Mg/Ca which does not necessarily stem from contaminant loss (Barker et al., 2003; Hasenfratz et al., 2017) and therefore was not applied in this study.

Fe/Ca and Mn/Ca ratios were used to assess sample contamination, whereby if contamination was a factor, it would be indicated by a covariance and a positive correlation between Mg/Ca and Fe/Ca and/or Mn/Ca (Barker et al., 2003). Figure 2a,b show downcore Mg/Ca results compared to Fe/Ca and Mn/Ca from the same samples for site MD01-2444 *G. affinis* analyses. There is no clear covariance of downcore records or significant correlation between Mg/Ca and Fe/Ca or Mn/Ca (Fig. 2). Al/Ca was below the limit of detection for most samples or very low. We thus consider diagenetic and clay contamination to have negligible effects on our Mg/Ca data, and all the samples were used in the final dataset.

https://doi.org/10.5194/egusphere-2026-3334
Preprint. Discussion started: 22 June 2026

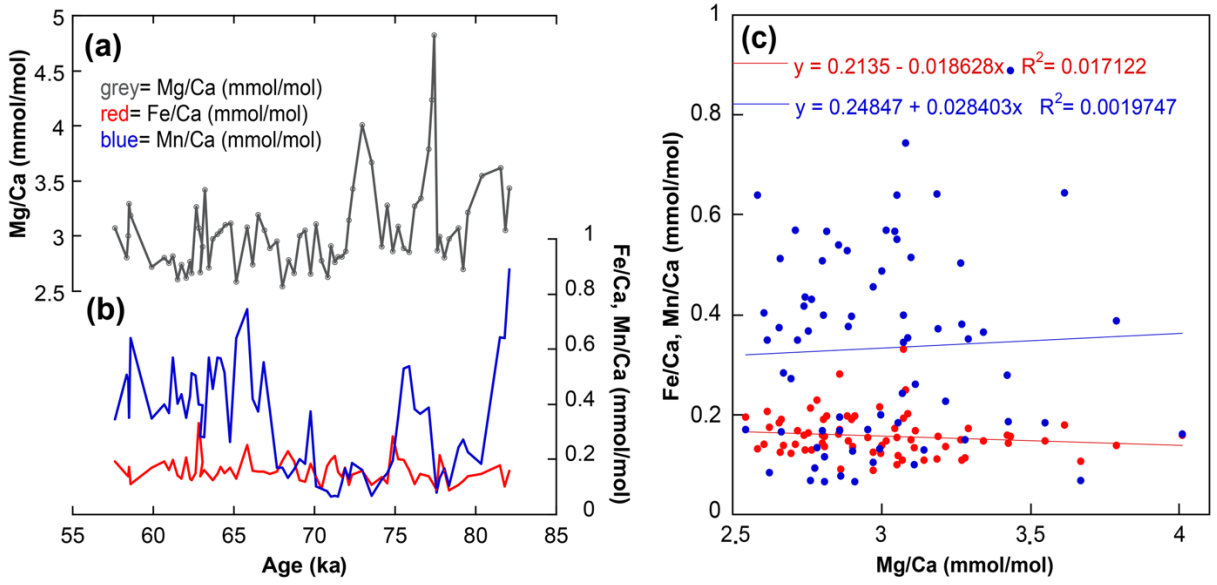

Figure 2. Contamination assessment of *G. affinis* Mg/Ca. (a, b) downcore records of Mg/Ca (grey), Mn/Ca (blue) and Fe/Ca (red); (c) cross plot of Mg/Ca (x-axis) versus Fe/Ca (red) and Mn/Ca (blue).

3.6 T_{dw} reconstructions

3.6.1 Calibration

Two calibrations exist to reconstruct T_{dw} from *G. affinis* Mg/Ca ratios. Here we use the core-top-based calibration of Weldeab et al. (2016a). Whilst this calibration is for reductively cleaned *G. affinis*, as opposed to oxidatively cleaned samples presented here, we refrain from applying additional "correction" factors to account for differences in cleaning protocols because the correction factors for *G. affinis* are not known, consistent with recent studies (Skinner et al., 2020; Thomas et al., 2025). The other available calibration of Skinner and Elderfield (2007) is a "pseudo calibration" based on a limited dataset of modern and past conditions *G. affinis* Mg/Ca measurements versus deep-water temperature constraints or temperatures being set to freezing limit during the LGM. The sensitivities of these two calibration options are very similar, implying that whilst the absolute temperature values might differ depending on the calibration chosen, the range of inferred T_{dw} variability (for the Mg/Ca range considered here) will only differ by 2%. In this study we place a greater emphasis on the observed trends of T_{dw} variability and the magnitude of change rather than on absolute temperature values obtained, which should be interpreted with caution (see sections 3.6.3 and 3.6.2).

3.6.2 Carbonate ion effects

Some studies have suggested that seawater carbonate ion, $[CO_3^{2-}]$, and/or calcite saturation state may act as a secondary parameter controlling benthic foraminiferal Mg/Ca with lower Mg/Ca when the carbonate ion saturation state is low (e.g.

https://doi.org/10.5194/egusphere-2026-3334
Preprint. Discussion started: 22 June 2026

Elderfield et al., 2010; Elderfield et al., 2006; Sadekov et al., 2014; Yu and Elderfield, 2008). However, this effect is particularly strong in epifaunal foraminifera such as *C. wuellerstorfi, C. mundulus* (e.g. Elderfield et al., 2006; Yu and Elderfield, 2008), or *Pyrgo* spp. (Sadekov et al., 2014). On the other hand, infaunal benthic foraminifera such as *Uvigerina* spp. and *G. affinis* are typically assumed to be less affected by bottom water $[CO_3^{2-}]$, because pore waters may quickly come to equilibration with respect to carbonate and thus the saturation state remains close to ~0 (Elderfield et al., 2010; Elderfield et al., 2006; Mawbey et al., 2020; Mawbey et al., 2026; Skinner et al., 2020; Skinner and Elderfield, 2007). However, a recent study showed that although $\Delta[CO_3^{2-}]$ of pore water is significantly lower than bottom water $\Delta[CO_3^{2-}]$, there can be a positive correlation between them, reflecting insufficient carbonate dissolution in the surface sediments (Weldeab et al., 2016a).

G. affinis has a relatively high temperature sensitivity implying that if present, any carbonate ion effects are secondary to T_{dw} changes (Weldeab et al., 2016a). We briefly consider the potential for $\Delta[CO_3^{2-}]$ influences on T_{dw} reconstructions at site MD01-2444. Weldeab et al. (2016a) report Mg/Ca sensitivity of 0.009±0.044 mmol/mol per μmol/kg change in $\Delta[CO_3^{2-}]$ for *G. affinis*. Although $\Delta[CO_3^{2-}]$ has not been reconstructed at the site of MD01-2444, a recent study used *C. wuellerstorfi* B/Ca measurements to reconstruct $\Delta[CO_3^{2-}]$ at nearby Iberian Margin site MD95-2039 (~3.4 km depth) (Yu et al., 2023). Yu et al. (2023) report a decrease in $[CO_3^{2-}]$ of ~25 μmol kg^{-1} at the MIS 5a/ 4 transition. This could have produced ~0.23 mmol/mol bias in Mg/Ca of *G. affinis*, equivalent to ~0.6°C decrease in T_{dw}, using the calibration of Weldeab et al. (2016a), as compared to the observed change in T_{dw} at the MIS 5a/4 transition of ~3°C. This implies a dominant temperature control on *G. affinis* Mg/Ca during this time interval.

The largest changes in Mg/Ca (and T_{dw}) at site MD01-2444 occur during MIS 5a Dansgaard-Oeschger (DO) stadial-interstadial changes, with reconstructed T_{dw} increases of 3-5°C during stadial events. Yu et al. (2023) report limited variability in $[CO_3^{2-}]$ during these abrupt events, implying that the Mg/Ca signal is likely primarily temperature driven. Even under a worst-case scenario, assuming ~ 30 μmol kg^{-1} changes in $\Delta[CO_3^{2-}]$ during stadials, as observed in the South Atlantic (Gottschalk et al., 2015; Lacerra et al., 2017), the resulting bias would amount to ~0.7°C.

3.6.3 T_{dw} Uncertainty Modelling

The uncertainty modelling approach used here is similar to that reported by Mawbey et al. (2026), making use of Monte Carlo (MC) modelling approach to probabilistically evaluate and quantify the uncertainty associated with the T_{dw} reconstruction. The ±2σ (i.e. 2 standard errors) of the T_{dw} dataset is 0.09 mmol/mol Mg/Ca, equivalent to ~0.3°C which is assumed to incorporate analytical error, proxy parameters uncertainties such as sampling uncertainties and random noise in the proxy signal. This was used as the tolerance for 10,000 MC iterations of T_{dw}, subsequently taking ±2σ standard deviation

https://doi.org/10.5194/egusphere-2026-3334
Preprint. Discussion started: 22 June 2026

of the 10,000 simulations as uncertainty for each sample (Fig. 3a). The mean overall uncertainty using this MC approach is ±0.3°C, which is smaller than the magnitude of any significant climatic variability reported in this study.

The uncertainty of the Weldeab et al. (2016a) calibration is ±1.6°C. Accordingly, we propagated the ±2σ uncertainty (i.e. 2 standard errors) of the dataset described above with the calibration uncertainty, to obtain ±1.7°C uncertainty tolerance which was fed into the MC model (10,000 iterations). The resulting ±1σ (standard deviation) mean is ±1°C (Fig. 3b).

Given the high calibration uncertainty, some of the variability in T_{dw} record falls within the error range of the MC analysis (Fig. 3b,c). This highlights the need for a cautious approach when interpreting absolute temperature values derived using the available reconstructions. In subsequent sections, calibration uncertainty is not propagated for the T_{dw} record; instead, error bars represent ±2σ standard deviation from MC modelling, based solely on ±2σ of the dataset (2 standard errors) tolerance. The *G. affinis* Mg/Ca record is retained on the T_{dw} "scale" to aid interpretation of the data.

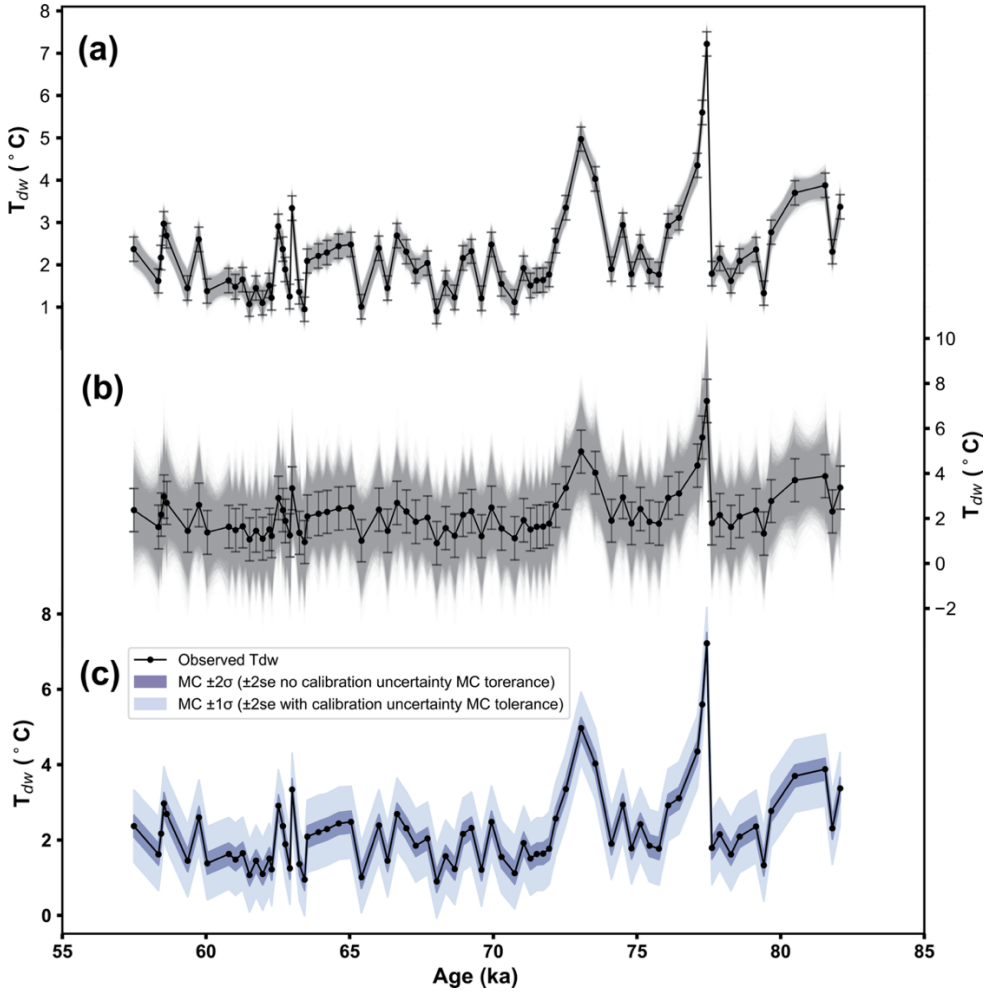

https://doi.org/10.5194/egusphere-2026-3334
Preprint. Discussion started: 22 June 2026

Figure 3. Uncertainty modelling of the deep-water temperature record. All panels show T_{dw} record (black lines) with different uncertainty modelling approaches (see text): (a) grey shading illustrates 10,000 MC simulations using ±2σ (2 standard errors) tolerance for the MC model excluding calibration uncertainty, error bars show ±2σ (standard deviation) of the MC simulations; (b) as for (a) but using propagated 2σ (s.e.) and calibration uncertainty for MC model tolerance, error bars showing ±1σ (standard deviation) of 10,000 MC simulations ; (c) the error intervals for the two different uncertainty modelling approaches illustrated in (a) and (b) with dark blue interval denoting ±2σ (standard deviation) of 10,000 MC simulations using ±2σ (2 standard errors) tolerance and excluding calibration uncertainty, whilst light blue confidence interval shows ±1σ (standard deviation) of 10,000 MC simulations using propagated ±2σ (2 standard errors) and calibration errors.

3.6.4 $\delta^{18}O_{dw}$ and $\delta^{18}O_{dw,anom}$ reconstructions

Here we combine *G. affinis* $\delta^{18}O$ (this study) with previously published *C. wuellerstorfi* $\delta^{18}O$ (Hodell et al., 2023). *C. wuellerstorfi* $\delta^{18}O$ was corrected by 0.64‰, and *G. affinis* $\delta^{18}O$ by -0.3‰, following Shackleton et al., (2000) and consistent with recent studies (e.g. Hodell et al., 2023; Thomas et al., 2025; Wharton et al., 2026) to correct for offsets from isotopic equilibrium (i.e. $\delta^{18}O$ of *Uvigerina* spp.).

To reconstruct $\delta^{18}O_{deep\text{-}water}$, $\delta^{18}O_{dw}$, paired $\delta^{18}O_{calcite}$ and *G. affinis* Mg/Ca-based temperature measurements were used, by solving the paleotemperature equation of Shackleton (1974) (Fig. 4c). A VPDB to VSMOW correction of 0.27‰ was applied. The combined benthic $\delta^{18}O$ record is generally of higher resolution than the *G. affinis* Mg/Ca, though interpolation was performed when $\delta^{18}O$ measurements were not available for an existing T_{dw} value (13 samples).

We apply two methods to isolate local hydrographic effects on $\delta^{18}O_{dw}$, e.g. as distinct from glacioeustatic effects arising from ice volume change (i.e. mean ocean $\delta^{18}O_{dw}$). The first involves subtracting an appropriately scaled relative sea level (RSL) component from the $\delta^{18}O$ records, which we denote $\delta^{18}O_{dw,local}$. This was achieved by assuming a benthic $\delta^{18}O$ change of ~1‰ for every 120m of sea level change (e.g. Shackleton, 2000; Shackleton et al., 2023; Waelbroeck et al., 2002) and using the RSL reconstruction of Rohling et al. (2008) (Fig. 4a,b). This approach incorporates uncertainties in RSL estimates and yields a record of anomalies relative to the global average signal. However, these anomalies may still partially reflect ice volume changes (Skinner and Shackleton, 2005), because meltwater requires time to be mixed into the global ocean. Consequently, the 'RSL related' component of any given $\delta^{18}O$ record will have a local expression that differs from the global mean, which in turn will lag ice volume change.

The second approach aims to isolate short term (millennial) variability by "subtracting" the long-term mean, which we denote $\delta^{18}O_{dw,anom}$. Here, a 6-ka moving mean window was used, following Cheng et al. (2017) and Siddall et al. (2010). Least-squares linear regression was carried out on 6ka windows centred on each data point, which allowed for a residual $\delta^{18}O$ to be calculated (Fig. 4a,b).

https://doi.org/10.5194/egusphere-2026-3334
Preprint. Discussion started: 22 June 2026

Figure 4a,b shows that both methods produce similar results, though we adopt the 6ka long-term mean method because it avoids the additional uncertainties associated with RSL reconstructions. Although the resulting time series is interpreted to primarily reflect local deep-water (hydrographic) variability, it should be noted that it may yet include the influence of unresolved millennial-scale meltwater inputs. Such variability has been proposed for MIS 3 based on sea-level reconstructions (e.g. Chappell, 2002; Siddall et al., 2003) but is not resolved in Rohling et al. (2008) RSL reconstruction or removed by using the 6-ka long-term mean method. No attempt is made to derive salinity estimates from $\delta^{18}O_{dw,anom}$ or $\delta^{18}O_{dw,local}$ due to the uncertainties involved, including in the $\delta^{18}O_{dw,local}$ -salinity relationship (Holloway et al., 2016; Rohling and Bigg, 1998).

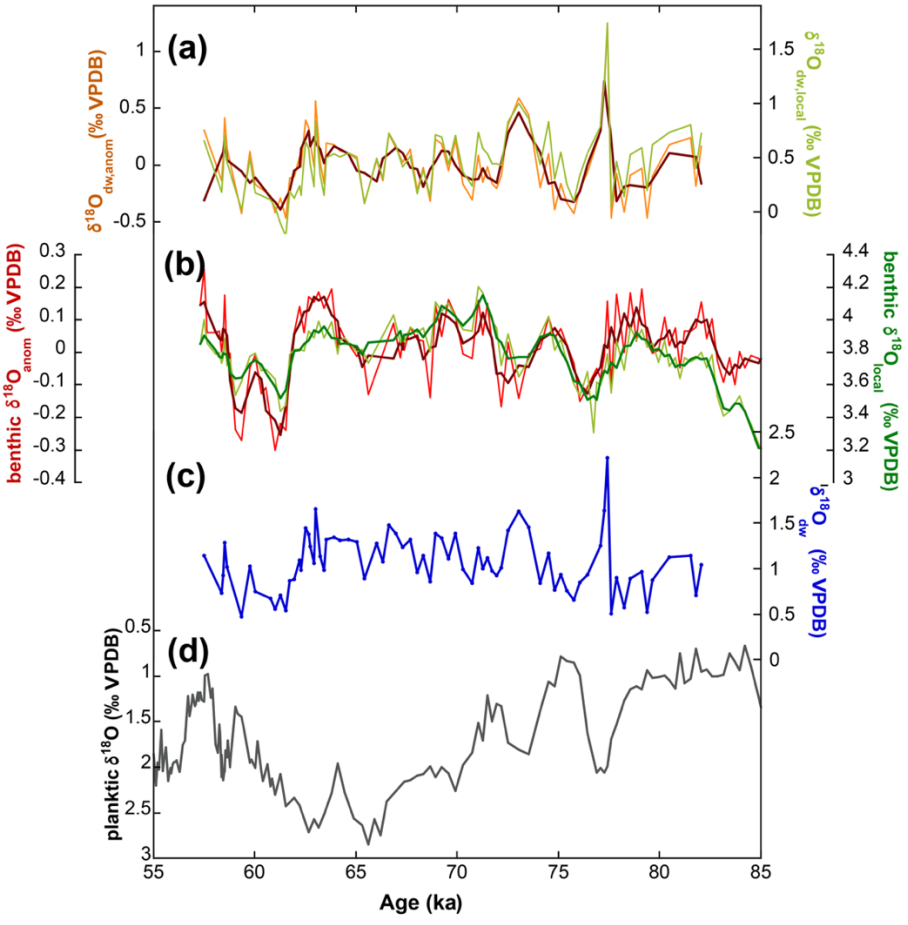

Figure 4. $\delta^{18}O_{dw}$ and $\delta^{18}O_{dw,anom/local}$ reconstruction methods. (a) $\delta^{18}O_{dw,anom}$ reconstructed using 6 ka moving average subtracted from $\delta^{18}O_{dw}$ (orange) and 3-point mean (brown) and $\delta^{18}O_{dw,local}$ subtracting RSL (Rohling et al., 2008) equivalent $\delta^{18}O$ from $\delta^{18}O_{dw}$ by assuming changes of ~1‰ for every 120 m of sea level (green); (b) as for (a) but detrending benthic $\delta^{18}O$ resulting in $\delta^{18}O_{anom}$ (red) and $\delta^{18}O_{local}$ (green); (c) derived $\delta^{18}O_{dw}$ by solving the paleotemperature equation of Shackleton (1974) using combined benthic $\delta^{18}O$ and *G. affinis* Mg/Ca-based temperatures (blue); planktic (*G. bulloides*) $\delta^{18}O$ (grey).

https://doi.org/10.5194/egusphere-2026-3334
Preprint. Discussion started: 22 June 2026

3.7 Sortable silt

Sample preparation was carried out following established protocols (Mccave et al., 1995; Mccave and Hall, 2006; Thornalley et al., 2018). Briefly, 150ml of 2M acetic acid was added to the entire dried fine fraction samples <63 μm (dried at <40ºC post sieving to prevent over-drying and sample degradation) and left to settle prior to excess acid being siphoned off. This step was repeated twice; subsequently rinsing with DI water and allowed to settle overnight. 200ml of freshly made 2M sodium carbonate was then added to remove organic matter, especially biosiliceous debris, and placed in a water bath at 85ºC for 5 hours (stirring every 2 hours), subsequently siphoned off and replaced with DI water which was left to settle. This DO rinse was repeated. Finally, DI water was replaced with 0.2% Calgon solution (sodium hexametaphosphate) to prevent aggregation. $\overline{SS}$ analyses were conducted on Coulter Counter Multisizer 3 at the Department of Geography, University College London. At least two separate aliquots were analysed for each sample.

Some samples (at a lower resolution than the $\overline{SS}$ record) were analysed for %SS using a Malvern Mastersizer 3000 laser diffraction particle size analyser at the Department of Geography, University College London. This was done to rule out contamination of the $\overline{SS}$ record by unsorted glacial silt (i.e. IRD) and make sure the fine sediments analysed have been sufficiently well current-sorted to provide a reliable flow history, following Mccave and Andrews (2019a); Mccave and Andrews (2019b), which was particularly important for this record because it spans HS 6. Figure 5b demonstrates a very strong correlation between %SS and $\overline{SS}$, with a running corelation mean of r =0.95 (Fig. 5a). This value is well above the threshold (r>0.5) proposed by Mccave and Andrews (2019b) to indicate well current-sorted sediment (Fig. 5a). It is therefore inferred that poor sorting, or 'contamination' by IRD (i.e. change in the sediment source signature, rather than sorting) is not the primary control on the $\overline{SS}$ record. A small number of samples around ~65 ka exhibited lower r values, although these remained above the r>0.5 threshold. Consequently, some caution should be exercised when interpreting the $\overline{SS}$ data within this interval. Importantly, no major changes are identified or interpreted in this study for this time period.

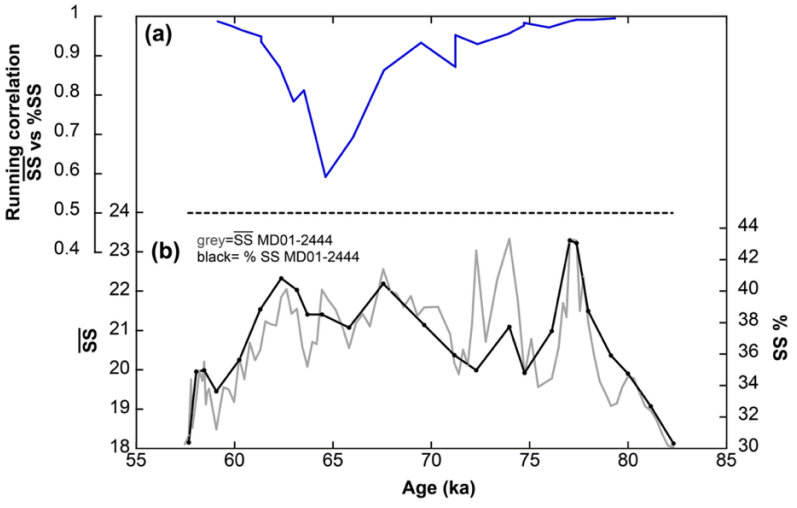

https://doi.org/10.5194/egusphere-2026-3334
Preprint. Discussion started: 22 June 2026

Figure 5. Sortable silt methods. (a) Running correlation between %SS and $\overline{SS}$ obtained from the Malvern particle size analyser (blue) and r = 0.5 correlation threshold (black dashed line); (b) comparison of %SS obtained from the Malvern particle size analyser (black) and $\overline{SS}$ obtained from the Coulter Counter(grey) (grey; arithmetic mean) records from site MD01-2444.

$\overline{SS}$ samples from Site ODP-1057 were originally reported by Evans et al. (2007) and re-analysed here using updated analytical procedures following e.g. Thornalley et al. (2018), on Coulter Counter Multisizer 3 at University College London.

4 Results

Based on the T_{dw}, $\delta^{18}O_{anom}$, $\delta^{18}O_{dw,anom}$ and $\overline{SS}$ records from site MD01-2444, three distinct deep-water hydrographic regimes are observed during the ~55-85 ka interval (Fig. 6).

1) An "interglacial", or warm circulation state during MIS 5a. Overall, a warmer baseline T_{dw} temperature persists throughout MIS 5a, punctuated by strong millennial perturbations. Very warm T_{dw} is observed during Greenland stadials C19 and C20 (Fig. 6e), accompanied by fast flow (Fig. 6f), low benthic $\delta^{18}O_{anom}$ (Fig. 6c) and elevated $\delta^{18}O_{dw,anom}$ (possibly indicative of saltier deep water). Meanwhile, the interstadials of MIS 5a were only marginally warmer than MIS 4 and/ or HS 6 glacial regimes, and potentially colder than the Holocene (with the caveat of relying on the temperature calibration).
2) The glacial "cold" circulation state during MIS 4 interval prior to HS6. This regime is characterised by generally cold T_{dw} in conjunction with relatively fast flow speed (Fig. 6e,f). T_{dw} appears to be colder than during the Holocene (again, given the calibration caveats), and colder than mean conditions during MIS 5a. On the MIS 5a/ 4 transition, there is a ~3°C decrease in T_{dw} from peak warmth during Greenland Stadial C19. Three millennial pulses are detected during early MIS 4 (green highlighting on Fig. 6). These are characterised by colder T_{dw}, lower benthic $\delta^{18}O_{anom}$ and $\delta^{18}O_{dw,anom}$.
3) A "Heinrich" mode during HS 6, characterised by cold T_{dw}. The observed variability during HS 6 can be split into two stages, whereby the observed T_{dw}, $\delta^{18}O_{anom}$, $\delta^{18}O_{dw,anom}$ and flow speeds decrease in the later stage (accompanied by increased benthic $\delta^{18}O$), whilst benthic $\delta^{13}C$ is low only in the earlier stage (Fig. 6).

https://doi.org/10.5194/egusphere-2026-3334
Preprint. Discussion started: 22 June 2026

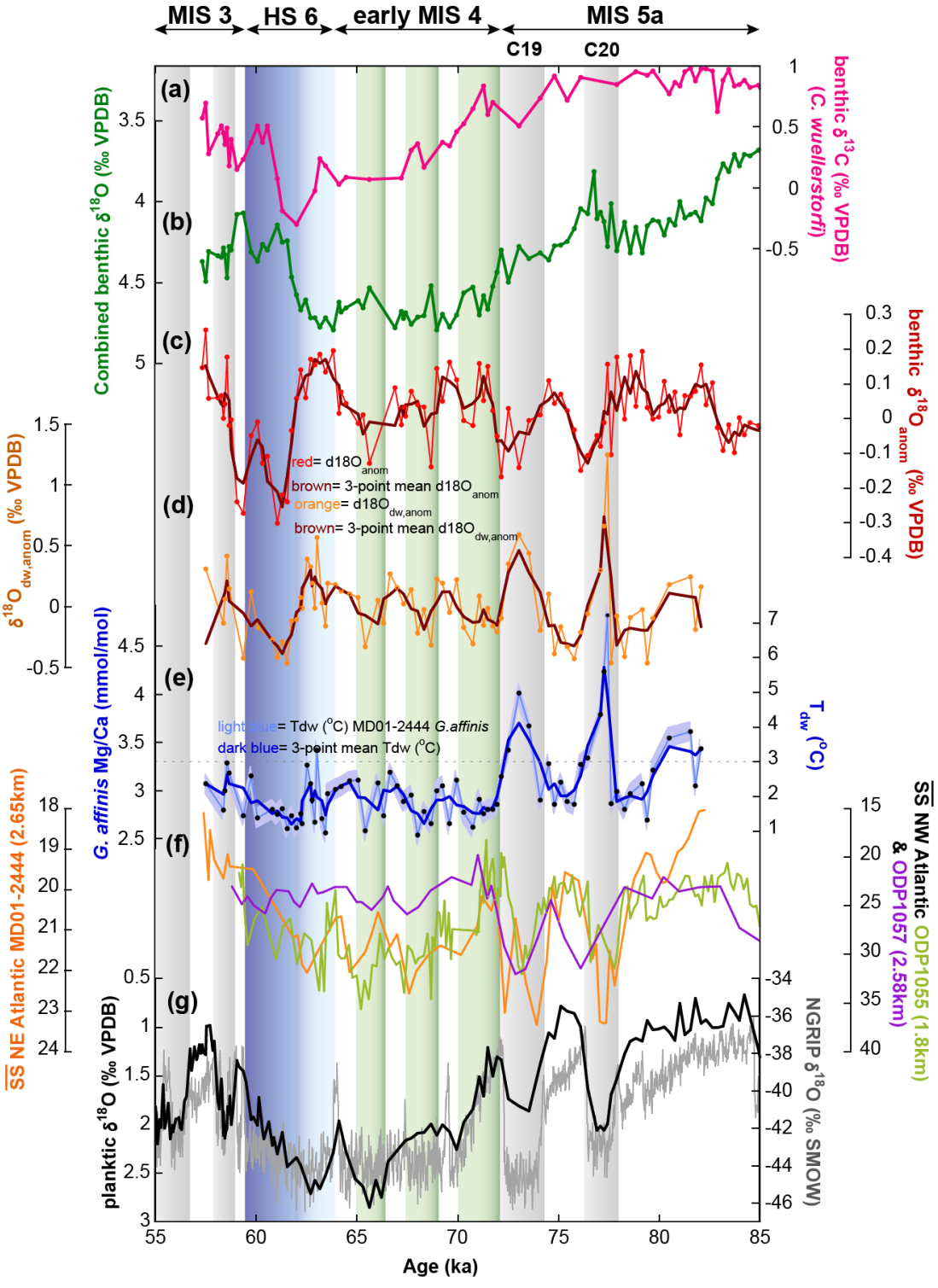

https://doi.org/10.5194/egusphere-2026-3334
Preprint. Discussion started: 22 June 2026

Figure 6. Deep-water hydrography reconstructions at North Atlantic site MD01-2444 (~2.65 km depth). (a) benthic $\delta^{13}C$ of *C. wuellerstorfi* (pink); (b) combined benthic $\delta^{18}O$ record of *C. wuellerstorfi* and *G. affinis* (green); (c) benthic $\delta^{18}O_{anom}$ (detrended combined benthic $\delta^{18}O$ record by subtracting 6 ka moving average method) (red) and 3-point mean (brown); (d) benthic $\delta^{18}O_{dw,anom}$ (detrended combined benthic $\delta^{18}O$ by subtracting out 6 ka moving average with temperature component removed using Mg/Ca-based T_{dw} reconstructions) (orange) and 3-point mean (brown); (e) *G. affinis* Mg/Ca and T_{dw} reconstructions using the calibration of Weldeab et al. (2016a) (light blue) and 3-point mean (dark blue), ±2σ (standard deviation) uncertainty intervals (blue shading) are derived using MC modelling with ±2σ (2 standard errors) tolerance and excluding calibration uncertainty (see section 3.6.3), black dashed line is 3°C showing modern and/or Holocene T_{dw} values (Hodell et al., 2014); (f) $\overline{SS}$ from NE Atlantic site MD01-2444 (orange) and $\overline{SS}$ from NW Atlantic sites ODP-1055 (light green) and ODP-1057 (purple) (Thornalley et al., 2013), note the reversed y-axis in this panel where stronger flow is at the bottom of the panel; (g) planktic (*G. bulloides*) $\delta^{18}O$ (black) and NGRIP $\delta^{18}O$ (grey) (Ngrip Project Members, 2004). Grey shading is used to highlight Greenland stadials during MIS 5a and MIS 3; green shading highlights colder episodes during early MIS 4; and blue shading represents HS 6, where the first part of the event is in light blue and the second part is dark blue. All records are presented on GICC05 timescale.

5 Discussion

In general, two mechanisms may have altered T_{dw} at site MD01-2444:

1) Under modern conditions, the site lies just above the boundary of southern-sourced water (LDW) and northern-sourced ENADW. Modern SSW is characterised by colder temperatures, and lower benthic $\delta^{18}O_{dw}$ and $\delta^{13}C$, than ENADW (e.g. Birner et al., 2016; Locarnini et al., 2024; Thomas et al., 2025). Thus, changes in water mass mixing and/ or the migration of LDW/ ENADW boundary in the past could potentially explain the hydrographic conditions recorded at site MD01-2444 (e.g. Skinner et al., 2007; Skinner et al., 2003).

In the modern Atlantic Ocean, NADW has higher $\delta^{18}O$ than Antarctic Bottom Water (AABW) because $\delta^{18}O$ is increased by evaporation but not by brine rejection. Today, modern datasets such as GLODAP and WOCE imply NADW temperatures of around 3°C in the Northeast Atlantic at ~2.6 km depth (Garcia et al., 2019; Garcia-Ibanez et al., 2015; Jenkins et al., 2015; Liu and Tanhua, 2021). While modern AABW temperature is estimated to be ~ -1 to 0°C (Johnson, 2008; Liu and Tanhua, 2021; Orsi et al., 1999; Rintoul et al., 2001), its modified derivative LDW (Liu and Tanhua, 2021) exhibits a temperature of ~2.5°C on the Iberian Margin (Hodell et al., 2014), in agreement with regional estimates ~2°C (Garcia-Ibanez et al., 2015; Liu and Tanhua, 2021; Van Aken, 2000).

2) Alternatively, changes in T_{dw} at the location of MD01-2444 may reflect changes in the temperature of the contributing endmembers. Previous work has suggested that past glacial-interglacial and stadial-interstadial changes were associated with shifts in the mode of operation of deep-water formation in the North Atlantic (e.g. Blaser et al., 2025; Repschlaeger et al., 2021; Stobbe et al., 2025; Wharton et al., 2026). At present, Nordic Seas overflow waters originate with temperatures <0°C, before being modified through entrainment to ~2-3°C (Dickson et al., 2002; Jochumsen et al., 2015), whereas LSW is substantially warmer, with characteristic temperatures of ~4-5°C (Yashayaev and Loder, 2016). Therefore, past changes in the source temperature of NADW endmembers and/ or shifts in the location(s) of deep-water formation/

https://doi.org/10.5194/egusphere-2026-3334
Preprint. Discussion started: 22 June 2026

convection could have propagated into the deep Northeastern Atlantic basin and contributed to the observed variability in T_{dw}.

5.1 Interglacial MIS 5a

High T_{dw} and $\delta^{18}O_{dw,anom}$ during MIS 5a stadials point to an incursion of a warm and saline deep-water mass during these events. T_{dw} was 3-5ºC warmer during C19 and 20 (Fig. 6e) than MIS 5a interstadials. Carbonate ion concentration changes have been shown to be negligible during these millennial events at nearby site MD95-2039 (Yu et al., 2023) thus could not have had much impact on *G. affinis* Mg/Ca. Nor can diagenetic or silicate contamination explain these changes, whereby neither Mn nor Fe (indicative of contamination) were elevated during these stadial events (Fig. 2). The T_{dw} changes observed are also much larger than our calculated 2σ uncertainty of ±0.3ºC (excluding calibration uncertainty) or 1σ uncertainty of ±1ºC (including the calibration uncertainty).

Subsurface warming at intermediate depths in the Atlantic has previously been reported during stadials (especially Heinrich stadials) from other proxy records (El Bani Altuna et al., 2021; Ezat et al., 2014; Marcott et al., 2011; Rasmussen et al., 2003; Sessford et al., 2019; Sessford et al., 2018; Weldeab et al., 2016b), and is apparent in 'hosing' modelling experiments (i.e. the subsurface warming is "a symptom" of AMOC weakening) (e.g. Alvarez-Solas et al., 2011; Clark et al., 2007; Galbraith et al., 2016; Knorr et al., 2021; Liu et al., 2009; Marcott et al., 2011; Pedro et al., 2018; Rühlemann et al., 2004; Vettoretti and Peltier, 2015; Zhang et al., 2017). However, all the proxy records which report the subsurface warming are derived from sites located at water depths shallower than 1.5 km in: the Nordic Seas (El Bani Altuna et al., 2021; Ezat et al., 2014; Rasmussen et al., 2003; Sessford et al., 2019; Sessford et al., 2018), Northwest Atlantic (Marcott et al., 2011) and the equatorial Atlantic (Weldeab et al., 2016b). Furthermore, the depth to which the subsurface warming penetrates in model simulations is model specific. Whilst some models indicate a subsurface warming above 2 km water depth (Brady and Otto-Bliesner, 2011; Clark et al., 2007; He et al., 2020; Knorr et al., 2021; Mignot et al., 2007; Rühlemann et al., 2004; Skinner et al., 2007) others show that the subsurface warming may extend deeper into the water column, particularly in the Northeast Atlantic reaching 2.5-3 km water depth, depending on model boundary conditions and parameterisations (Galbraith et al., 2016; Knorr et al., 2021; Liu et al., 2009; Marcott et al., 2011; Pedro et al., 2018; Vettoretti and Peltier, 2015). Given the evidence presented in these studies, an observed subsurface warming of the ocean interior reaching site MD01-2444 during MIS 5a stadials may be indicative of a weaker AMOC.

However, previous work suggests that typically, during glacial stadials, at site MD01-2444 there is an increase in SSW and an associated cooling of T_{dw} (Skinner and Elderfield, 2007). This is supported by other work reporting reduced T_{dw} during HS 1 from slightly deeper sites in the Northeast Atlantic (Repschläger et al., 2015; Skinner et al., 2003) likely due to the influence of SSW. Therefore, given that during MIS 5a stadials we observe a warming and no clear evidence of lower

https://doi.org/10.5194/egusphere-2026-3334
Preprint. Discussion started: 22 June 2026

benthic $\delta^{13}C$ (Fig. 6) to indicate increased influence of SSW, we propose that different dynamics were at play during MIS 5a stadials compared to glacial stadials of MIS 3.

In support of this concept, numerical modelling simulations by Knorr et al. (2021) illustrate that subsurface warming during AMOC weakening ('hosing') experiments reaches ~2.5 km water depth at ~40°N under interglacial boundary conditions, but only to ~2 km depth at the same latitude under LGM boundary conditions due to a shallower NADW cell under glacial boundary conditions. Thus, the character of T_{dw} changes at the site of MD01-2444, associated with AMOC perturbations, is expected to depend on the background climate regime.

However, the observed warmings during MIS 5a stadials may not reflect a standard 'stagnation warming' effect arising from a 'collapsed' AMOC (or more specifically NADW weakening). This is because the MD01-2444 flow speed $\overline{SS}$ record, as well as reconstructions of the strength of the upper 3 km of DWBC in the western North Atlantic (Thornalley et al., 2013), both suggest significantly stronger flow during MIS 5a stadials, in parallel with elevated T_{dw} (Fig. 6f), which is difficult to reconcile with a reduction in deep water formation to these depths that would be necessary to cause a subsurface warming.

The tight coupling observed between the $\overline{SS}$ records from MD01-2444 and sites ODP-1055 (~1.8 km depth) and ODP-1057 (~2.6 km depth) in the Northwest Atlantic (Fig. 6f) (Thornalley et al., 2013) suggests synchronous changes in circulation strength occurred simultaneously in the Northwest and Northeast Atlantic, at least at the location of these three sites. The NW Atlantic sites are too shallow to have experienced significant influence from SSW, even during glacial conditions (e.g. Blaser et al., 2020; Blaser et al., 2025; Howe et al., 2016; Pöppelmeier et al., 2020; Pöppelmeier et al., 2018; Thornalley et al., 2013; Wharton et al., 2026). Additionally, no reductions in benthic $\delta^{13}C$ – an indicator of increased SSW influence - are observed at these sites during MIS 5a stadials (Evans et al., 2007; Thornalley et al., 2013). Therefore, the flow changes they record are considered most likely of northern origin. The covariation between records from the NW Atlantic sites and site MD01-2444 suggests that MIS 5a changes observed in the NE Atlantic at ~2.65 km were linked to variability in the properties and dynamics of NADW.

One mechanism that may explain the warmer, more saline deep water and stronger flow during MIS 5a stadials at the Iberian Margin is a southward shift in North Atlantic convection sites. Today, deep water masses form in the subpolar North Atlantic by open ocean convection and entrainment (Petit et al., 2020). Convection occurs in the Nordic Seas, south of Greenland-Scotland Ridge in the Irminger and Icelandic Basins, and to a lesser extent in the Labrador Sea (Petit et al., 2020). During Greenland stadials, atmospheric cooling (Ngrip Project Members, 2004) likely promoted an expansion of sea ice at high northern latitudes (El Bani Altuna et al., 2024; Hoff et al., 2016; Sadatzki et al., 2019) that may have inhibited open ocean convection and displaced convection sites southward. This may have produced warmer and more saline NSW source waters, generating a distinct mode of NADW that was subsequently advected into the mid-depth, midlatitude North Atlantic.

https://doi.org/10.5194/egusphere-2026-3334
Preprint. Discussion started: 22 June 2026

Notably, although Greenland appears cold during C19 and C20, relatively warm surface ocean conditions persisted across both the midlatitude North Atlantic (e.g. Voelker and De Abreu, 2011; Zeng et al., 2023) and the subpolar North Atlantic between ~50-60°N (Barker et al., 2015; Bauch et al., 2012; Mcmanus et al., 1994; Thornalley et al., 2013; Zeng et al., 2025) until the onset of MIS 4 (~72 ka), as reflected by the delayed increase of % *N. pachyderma.* These low abundances further suggest that sea ice did not extend sufficiently far south to supress convection throughout the subpolar North Atlantic, potentially allowing continued NADW formation at more southerly sites during these stadials.

Several mechanisms have been proposed to explain glacial NADW formation during stadials, likely associated with southward-shifted convection sites (Blaser et al., 2025; Sherriff-Tadano et al., 2018; Wharton et al., 2026). Low $\delta^{18}O_{anom}$ values (i.e. benthic foraminifera $\delta^{18}O$ "corrected" for global ice volume effect), such as those observed at MD01-2444 during C19 and C20 (Fig. 6c), may result either from reduced $\delta^{18}O_{dw}$ linked to isotopically light meltwater and/ or changes in salinity, or from elevated deep-water temperatures. Earlier studies largely favoured the former mechanism, whereby enhanced sea-ice formation led to brine rejection, increasing surface salinity and promoting deep water convection from isotopically light meltwater (e.g. Dokken and Jansen, 1999; Farmer et al., 2023; Thornalley et al., 2010). Under this scenario, T_{dw} would likely have remained stable or decreased.

In contrast, the observed low $\delta^{18}O_{anom}$ values at site MD01-2444 appear to be associated with elevated temperature (Fig. 6e). However, the origin of this warming remains debated. One possibility is that warming occurred alongside relatively low $\delta^{18}O_{dw}$ waters influenced by freshwater input and meltwater incorporation, as proposed by e.g. Zhang et al. (2017). Alternatively, and more consistent with the observations presented here, elevated temperatures coincide with high $\delta^{18}O_{dw, anom}$ values (Fig. 6d), implying relatively saline source waters. This interpretation supports mechanisms invoking warm, saline deep-water formation south of the expanded sea-ice margin, potentially involving enhanced mixing with the subtropical Atlantic (Blaser et al., 2025), the Mediterranean (Repschlaeger et al., 2021) and/or more salty glacial North Atlantic Current (NAC) (Sherriff-Tadano et al., 2018; Wharton et al., 2026). A higher salinity would imply less cooling was required for deep convection, facilitating continued NADW formation at more southerly convection locations. Consistent with this interpretation, a recent numerical modelling simulation forced with boundary conditions broadly similar to MIS 5a, albeit with lower atmospheric CO_2 (CO_2 <180ppm, low obliquity and pre-industrial ice sheet configuration), yielded an unusually warm and salty NADW, resulting from a southward shift in convection sites linked to an expansion of sea ice (Galbraith and De Lavergne, 2019).

Although the pulses of warm, salty, fast-flowing deep water observed during MIS 5a stadials might be interpreted to indicate an increased influence of MOW at site MD01-2444 - consistent with evidence for a deeper and stronger MOW core across the MIS 5a/4 transition (Chen et al., 2025; Nichols et al., 2020) and during the LGM (Rogerson et al., 2005) – this

https://doi.org/10.5194/egusphere-2026-3334
Preprint. Discussion started: 22 June 2026

interpretation is inconsistent with the absence of elevated benthic $\delta^{13}C$ (>1‰) during MIS 5a stadials (Repschlaeger et al., 2021; Schönfeld and Zahn, 2000; Voelker et al., 2006; Zahn et al., 1987) (Fig. 6a).

We therefore infer that the subsurface warmings observed at the Iberian Margin during MIS 5a stadials most likely reflect changes in deep water source regions in the subpolar in North Atlantic. This would imply that ocean circulation and AMOC responses differed during MIS 5a stadials and glacial stadials of MIS 3, and that the nature of AMOC variability is strongly dependent on background climate conditions. In particular, the data support continuous vigorous circulation of the northern sourced waters within the upper ~3 km of the North Atlantic during C19 and C20, consistent with findings of Thornalley et al. (2013).

5.2 Glacial MIS 4

The glacial (pre-HS 6) MIS 4 T_{dw} was generally cold, and likely colder than Holocene and MIS 5a; Fig. 6). The mean MIS 4 (~63.5-72 ka) T_{dw} is 1.9±0.3ºC, which is comparable to 1.9±0.5ºC temperature observed in the northwest Atlantic during the LGM based on *G. affinis* Mg/Ca (Wharton et al., 2026). Although these absolute T_{dw} values should be interpreted with caution (see above), these two values are comparable because they make use of Mg/Ca derived T_{dw} from the same species and calibration, albeit slight differences in the cleaning protocols. This would suggest a similar deep-water temperature during the LGM and MIS 4, supporting previous studies that have suggested similar hydrography (Adkins, 2013; Barker and Diz, 2014; Martrat et al., 2007; Piotrowski et al., 2005; Stobbe et al., 2025; Thornalley et al., 2013; Yu et al., 2023).

Recalibrated *G. affinis* Mg/Ca from nearby Iberian Margin site MD99-2334K (~3.2 km) of Skinner et al. (2003) and (Skinner et al., 2007) (using the calibration of Weldeab et al. (2016a)) yield an LGM T_{dw} mean of 0.9ºC (~20-24 ka). This estimate is ~1ºC colder than T_{dw} observed during MIS 4, possibly due to a greater influence of SSW at this site and in the NE Atlantic during the LGM than at the site of MD01-2444 during MIS 4 (Chalk et al., 2019; Skinner et al., 2021; Stobbe et al., 2025). However, Wharton et al. (2026) report that the observed LGM deep-water temperature in the northwest Atlantic can be explained solely by changes in northern-sourced waters, without requiring additional influence from SSW. Other studies have also argued for continuous production and influence of NSW in the NW Atlantic at the LGM (e.g. Blaser et al., 2020; Blaser et al., 2025; Pöppelmeier et al., 2021; Stobbe et al., 2025; Wharton et al., 2026). At present, it remains unclear to what extent NSW and SSW have influenced the Iberian Margin during MIS4, and if this was different to the LGM.

In addition to cold T_{dw} during MIS 4, faster flow is seen at site MD01-2444 during early MIS 4, as well as NW Atlantic site ODP-1055 (Fig. 6f). The fast flow at site ODP-1055 has previously been interpreted to reflect the shoaled Deep Western Boundary Current/ NADW, whereby the $\overline{SS}$ record from a deeper NW Atlantic site ODP-1059 (~3 km depth) showed a distinct weakening of circulation at the MIS 5a/ 4 transition (Thornalley et al., 2013). The transport rate of MIS 4 AMOC is poorly constrained; therefore, we consider transport changes during the LGM, assuming broadly similar glacial circulation

https://doi.org/10.5194/egusphere-2026-3334
Preprint. Discussion started: 22 June 2026

states. Modelling studies disagree on the strength (and spatial extent) of the LGM AMOC/ NADW under glacial boundary conditions, with some models showing a strong LGM AMOC. This may reflect stronger cooling under glacial boundary conditions, which enhances convection, and/ or higher glacial topography of the Laurentide Ice Sheet (LIS), which could have strengthened North Atlantic westerlies through atmospheric circulation steering (e.g. Galbraith and De Lavergne, 2019; Kageyama et al., 2021; Klockmann et al., 2016; Sherriff-Tadano et al., 2018). These simulations further show that stronger glacial winds lead to increased convection in the Labrador Sea, Icelandic and Irminger Basins (Klockmann et al., 2016; Sherriff-Tadano et al., 2018), or alternatively stronger convection in the Labrador Sea while reducing convection in parts of the Icelandic and Irminger Basins (Galbraith and De Lavergne, 2019). Additionally, modelling experiments by (Menviel et al., 2020) suggest that under LGM boundary conditions, even a weaker overall AMOC may be associated with stronger flow on the eastern side of the Mid-Atlantic Ridge.

NW site ODP-1055 is directly under the influence of LSW, whilst NE Atlantic site MD01-2444 is under the influence of ENADW, made up of ~45% of LSW (Jenkins et al., 2015; Thomas et al., 2022). Thus, we propose that both sites record changes in LSW strength that have been propagated to the mid-depth midlatitude North Atlantic in the western and eastern basins. The stronger convection in the Labrador Sea, and south of Greenland-Scotland ridge (i.e. Irminger and Icelandic Basins) and/ or a glacial southward shift of convection sites may have increased LSW strength without necessarily changing the mean transport of NADW/ AMOC, which instead might have even been weaker overall due to decreased convection in the Nordic Seas for example, linked to expanded glacial sea ice. This would imply a continued influence of NSW at site MD01-2444 during early MIS 4.

Meanwhile, the observed millennial pulses during MIS 4, characterised by colder T_{dw}, lower benthic $\delta^{18}O_{anom}$ and $\delta^{18}O_{dw,anom}$ (implying reduced salinity), may reflect either increased SSW incursions at the site (Skinner and Elderfield, 2007), or changes in the type and amount of different modes of NSW (Blaser et al., 2025). However, the former mechanism is favoured, as the MIS 4 millennial variability closely resembles that identified by Skinner and Elderfield (2007) during MIS 3 at the same core site, both in terms of the magnitude of temperature change (~1-1.5ºC for non-Heinrich Stadials), and the sense of change (i.e. colder and less saline during intervals of SSW incursions). Although these pulses are not clearly expressed in the benthic $\delta^{13}C$ record (Fig. 6a), this likely reflects the relatively low resolution of $\delta^{13}C$ record. It is also unlikely that the observed variability is an artefact as it is replicated by multiple proxy records, including the T_{dw}, $\delta^{18}O_{anom}$ and $\delta^{18}O_{dw,anom}$ records, whereby T_{dw} and $\delta^{18}O_{anom}$ are independent proxies. To our knowledge, this type of millennial variability has not been previously detected during MIS 4 in Greenland or Antarctic ice core isotope records, nor in atmospheric CO_2. Nevertheless, these "cold" pulses tentatively coincide with intervals of expanded Southern Ocean sea ice and elevated Antarctic ice core $\delta^{13}C_{CO2}$ (Menking et al., 2022; Wolff et al., 2006).

https://doi.org/10.5194/egusphere-2026-3334
Preprint. Discussion started: 22 June 2026

In summary, the Northeast Atlantic (Iberian Margin) mid-depth circulation during early (pre-HS 6) MIS 4 differed from both the interglacial conditions of MIS 5a and the more extreme conditions of HS 6 but was broadly similar to the LGM. Both southern- and northern-sourced waters may have influenced site MD01-2444 during this time interval.

5.3 Heinrich Stadial 6 (HS 6)

The third hydrographic/ circulation regime is observed during HS 6, which represents a major change in deep North Atlantic circulation, as inferred from reduced T_{dw}, very low benthic $\delta^{13}C$, $\delta^{18}O_{anom}$, and $\delta^{18}O_{dw,anom}$, and reduced flow speed. Together, these changes point to the influence of SSW. A number of proxy records have been used to suggest a much weaker circulation in the Atlantic and a clear influence of SSW below ~2 km during HS 6 (Böhm et al., 2015; Hall and Mccave, 2000; Piotrowski et al., 2005; Thornalley et al., 2013; Yu et al., 2016), similar to HS 1 (e.g. Böhm et al., 2015; Hoogakker et al., 2015; Mcmanus et al., 2004; Ng et al., 2018; Skinner et al., 2021; Skinner et al., 2003). Some recent studies have emphasised that active deep-water formation persisted in the North Atlantic during HS 1, transporting "Heinrich-modified" NADW to depths (e.g. Blaser et al., 2025; Repschlaeger et al., 2021). Yet, the very low $\delta^{13}C$ and low T_{dw} observed at the Iberian Magin in this study for HS 6, and HS 1 (Skinner et al., 2003), HS 4 and 5 (Skinner et al., 2007; Skinner and Elderfield, 2007), alongside reduced deep-water oxygen concentration (Hoogakker et al., 2015) and higher radiocarbon ventilation ages (Skinner et al., 2021) have been interpreted as evidence for SSW incursions below ~2 km at the Iberian Margin during Heinrich Stadials.

The "two-stage" HS 6 variability observed in this study (Fig. 6) is characterised by low T_{dw}, $\delta^{18}O_{anom}$, and $\delta^{18}O_{dw,anom}$ and flow speed in the later part; whilst benthic $\delta^{13}C$ appears low only in the first half of the stadial. The stadial is marked by a brief, yet significant, T_{dw} increase approximately mid-way between the two phases. The concept of multiple phases during a single Heinrich Stadial has been previously reported by proxy studies (e.g. Bard et al., 2000; Broecker and Putnam, 2012; Campos et al., 2025a; Campos et al., 2025b; Crivellari et al., 2018; Gherardi et al., 2005; Hodell et al., 2017; Huang et al., 2014; Jena et al., 2026; Margari et al., 2020; Peck et al., 2007; Robinson et al., 2005; Singh et al., 2023; Skinner and Elderfield, 2007; Thornalley et al., 2011; Tzedakis et al., 2018; Wendt et al., 2019; Yu et al., 2023; Zhang et al., 2014) and modelling studies (Ziemen et al., 2019). Especially noteworthy is the T_{dw} variability observed by Skinner and Elderfield (2007) at site MD01-2444 during HS 4 and HS 5, which is consistent with the mid-stadial temperature increase observed during HS 6. It remains difficult to disentangle the drivers of these changes in deep-water temperature. Previous studies have suggested centennial-scale variability in AMOC during Heinrich Stadials (Campos et al., 2025b; Jena et al., 2026; Skinner and Elderfield, 2007; Thornalley et al., 2015; Thornalley et al., 2011; Tzedakis et al., 2018), which may account for the variability observed during HS 6. Thus, observations presented here support for possibility of sub-millennial variability during Heinrich Stadials, highlighting the complexity of deep-water circulation dynamics.

https://doi.org/10.5194/egusphere-2026-3334
Preprint. Discussion started: 22 June 2026

6 Conclusions

Three distinct deep-water hydrographic 'regimes' are identified at the Iberian Margin site MD01-2444 (~2.65 km) over the ~55-85 ka interval: 1) an "interglacial", or warm circulation mode during MIS 5a; 2) the glacial "cold" circulation mode during pre-HS 6 MIS 4; and 3) a more severe "Heinrich" mode during HS 6. These are broadly analogous to the circulation configurations proposed for the Holocene, the LGM and HS 1, respectively, thus mirroring patterns observed during the deglaciation (Lynch-Stieglitz, 2017; Rahmstorf, 2002), albeit in the absence of a glacial 'Termination'.

We suggest that local oscillations in North Atlantic T_{dw} are governed by a combination of changing SSW contribution, and changing temperature in deep-water formation source regions in the high-latitude North Atlantic. Regime one (interglacial MIS 5a) is characterised by millennial-scale intervals of warm T_{dw}, saline waters and fast flow, occurring during Greenland stadials C19 and C20. We attribute these conditions to a southward displacement of convection sites in the North Atlantic (e.g. south of Iceland). Subsurface warming during these stadials may extend to at least ~2.65 km depth in the North Atlantic, albeit via different processes than posited previously for AMOC collapse (e.g. Alvarez-Solas et al., 2011; El Bani Altuna et al., 2021; Knorr et al., 2021; Marcott et al., 2011; Winton and Sarachik, 1993). Our results suggest that the mode and magnitude of subsurface heat budget variability in the North Atlantic, and associated AMOC responses, strongly depends on the background climate state.

Regime two (pre-HS 6 MIS 4), exhibits millennial variability, likely reflecting intermittent to SSW influence at the Iberian Margin, potentially driven by changes in Southern Ocean sea-ice against a backdrop of strengthened LSW and a persistent influence of NSW throughout MIS 4. During regime three ("Heinrich mode" during HS 6), colder T_{dw} and a pronounced SSW signal dominate the record. This interval appears to be expressed as a two-stage event, consistent in some respects with the structure of other Heinrich events (Bard et al., 2000; Hodell et al., 2017; Skinner and Elderfield, 2007).

Overall, our findings emphasize similarities between the MIS4/3 and MIS1/2 transitions, despite their very different implications for global ice volume. However, we also show that the same mode of millennial DO-type variability may be associated with very different impacts on deep-water hydrography and circulation strength in the North Atlantic, depending on the background state, with clear differences between the expression of millennial events in the deep ocean between MIS 3, 4, and 5.

https://doi.org/10.5194/egusphere-2026-3334
Preprint. Discussion started: 22 June 2026

Data availability

New data are archived and available at PANGAEA: http://XX and http://XX. Chronology for site MD01-2444 is available at http://XX.

Supplement link

N/A.

Author contributions

S.R. and L.C.S. conceived and designed the study. S.R. generated all the records together with M.G. for foraminiferal trace metal analyses and D.J.R.T. for sortable silt analyses. S.R. analysed and interpreted the data, and wrote the manuscript, with contributions from all authors.

Competing interests

Two of the (co-)authors are members of the editorial board of Climate of the Past. The authors declare that they have no other competing interests.

Disclaimer

Publisher's note:

Acknowledgements

S.R. acknowledges the financial support of NERC studentship 2073288. D.T. acknowledges funding from the Leverhulme Trust.

Review statement

tbc

https://doi.org/10.5194/egusphere-2026-3334
Preprint. Discussion started: 22 June 2026

References

Adkins, J. F.: The role of deep ocean circulation in setting glacial climates, Paleoceanography, 28, 539-561, 10.1002/palo.20046, 2013.

Alvarez-Solas, J., Montoya, M., Ritz, C., Ramstein, G., Charbit, S., Dumas, C., Nisancioglu, K., Dokken, T., and Ganopolski, A.: Heinrich event 1: an example of dynamical ice-sheet reaction to oceanic changes, Climate of the Past, 7, 1297-1306, 10.5194/cp-7-1297-2011, 2011.

Bard, E., Rostek, F., Turon, J.-L., and Gendreau, S.: Hydrological impact of Heinrich events in the subtropical northeast Atlantic, Science, 289, 1321-1324, 2000.

Barker, S. and Diz, P.: Timing of the descent into the last Ice Age determined by the bipolar seesaw, Paleoceanography, 29, 489-507, 10.1002/2014pa002623, 2014.

Barker, S., Greaves, M., and Elderfield, H.: A study of cleaning procedures used for foraminiferal Mg/Ca paleothermometry, Geochemistry Geophysics Geosystems, 4, 10.1029/2003gc000559, 2003.

Barker, S., Chen, J., Gong, X., Jonkers, L., Knorr, G., and Thornalley, D.: Icebergs not the trigger for North Atlantic cold events, Nature, 520, 333-336, 2015.

Batchelor, C. L., Margold, M., Krapp, M., Murton, D. K., Dalton, A. S., Gibbard, P. L., Stokes, C. R., Murton, J. B., and Manica, A.: The configuration of Northern Hemisphere ice sheets through the Quaternary, Nature communications, 10, 3713, 2019.

Bauch, H. A., Kandiano, E. S., and Helmke, J. P.: Contrasting ocean changes between the subpolar and polar North Atlantic during the past 135 ka, Geophysical Research Letters, 39, 2012.

Bereiter, B., Lüthi, D., Siegrist, M., Schüpbach, S., Stocker, T. F., and Fischer, H.: Mode change of millennial CO₂ variability during the last glacial cycle associated with a bipolar marine carbon seesaw, Proceedings of the National Academy of Sciences of the United States of America, 109, 9755-9760, 10.1073/pnas.1204069109, 2012.

Birner, B., Hodell, D., Tzedakis, P., and Skinner, L.: Similar millennial climate variability on the Iberian margin during two early Pleistocene glacials and MIS 3, Paleoceanography, 31, 203-217, 2016.

Blaser, P., Gutjahr, M., Pöppelmeier, F., Frank, M., Kaboth-Bahr, S., and Lippold, J.: Labrador Sea bottom water provenance and REE exchange during the past 35,000 years, Earth and Planetary Science Letters, 542, 10.1016/j.epsl.2020.116299, 2020.

Blaser, P., Waelbroeck, C., Thornalley, D. J. R., Lippold, J., Pöppelmeier, F., Kaboth-Bahr, S., Repschläger, J., and Jaccard, S. L.: Prevalent North Atlantic Deep Water during the Last Glacial Maximum and Heinrich Stadial 1, Nature Geoscience, 18, 410-416, 10.1038/s41561-025-01685-5, 2025.

Böhm, E., Lippold, J., Gutjahr, M., Frank, M., Blaser, P., Antz, B., Fohlmeister, J., Frank, N., Andersen, M. B., and Deininger, M.: Strong and deep Atlantic meridional overturning circulation during the last glacial cycle, Nature, 517, 73-U170, 10.1038/nature14059, 2015.

Boyle, E. A. and Keigwin, L. D.: COMPARISON OF ATLANTIC AND PACIFIC PALEOCHEMICAL RECORDS FOR THE LAST 215,000 YEARS - CHANGES IN DEEP OCEAN CIRCULATION AND CHEMICAL INVENTORIES, Earth and Planetary Science Letters, 76, 135-150, 10.1016/0012-821x(85)90154-2, 1985.

Bradtmiller, L. I., McManus, J. F., and Robinson, L. F.: 231Pa/230Th evidence for a weakened but persistent Atlantic meridional overturning circulation during Heinrich Stadial 1, Nature Communications, 5, 10.1038/ncomms6817, 2014.

Brady, E. C. and Otto-Bliesner, B. L.: The role of meltwater-induced subsurface ocean warming in regulating the Atlantic meridional overturning in glacial climate simulations, Climate Dynamics, 37, 1517-1532, 10.1007/s00382-010-0925-9, 2011.

Broecker, W. and Putnam, A. E.: How did the hydrologic cycle respond to the two-phase mystery interval?, Quaternary Science Reviews, 57, 17-25, 10.1016/j.quascirev.2012.09.024, 2012.

Brovkin, V., Ganopolski, A., Archer, D., and Munhoven, G.: Glacial CO 2 cycle as a succession of key physical and biogeochemical processes, Climate of the Past, 8, 251-264, 2012.

Campos, M. C., Chiessi, C. M., Nascimento, R. A., Kraft, L., Radionovskaya, S., Skinner, L., Dias, B. B., Pinho, T. M., Kochhann, M. V., and Crivellari, S.: Millennial-to centennial-scale Atlantic ITCZ swings during the penultimate deglaciation, Quaternary Science Reviews, 348, 109095, 2025a.

https://doi.org/10.5194/egusphere-2026-3334
Preprint. Discussion started: 22 June 2026

Campos, M. C., Nascimento, R. A., Pinho, T. M., Kraft, L., Crivellari, S., Radionovskaya, S., Skinner, L., Dias, B. B., Portilho-Ramos, R. C., and Hartmann, G. A.: Two-phased ITCZ-driven upper salinity stratification in the western equatorial Atlantic during Heinrich Stadial 11, Global and Planetary Change, 105119, https://doi.org/10.1016/j.gloplacha.2025.105119, 2025b.

Chalk, T. B., Foster, G. L., and Wilson, P. A.: Dynamic storage of glacial CO2 in the Atlantic Ocean revealed by boron CO32- and pH records, Earth and Planetary Science Letters, 510, 1-11, 10.1016/j.epsl.2018.12.022, 2019.

Chappell, J.: Sea level changes forced ice breakouts in the Last Glacial cycle: new results from coral terraces, Quaternary Science Reviews, 21, 1229-1240, 2002.

Cheng, H., Edwards, R. L., Sinha, A., Spötl, C., Yi, L., Chen, S. T., Kelly, M., Kathayat, G., Wang, X. F., Li, X. L., Kong, X. G., Wang, Y. J., Ning, Y. F., and Zhang, H. W.: The Asian monsoon over the past 640,000 years and ice age terminations (vol 534, pg 640, 2016), Nature, 541, 122-122, 10.1038/nature20585, 2017.

Clark, P. U., Hostetler, S. W., Pisias, N. G., Schmittner, A., and Meissner, K. J.: Mechanisms for an~ 7-kyr climate and sea-level oscillation during marine isotope stage 3, Ocean circulation: Mechanisms and impacts—past and future changes of meridional overturning, 173, 209-246, 2007.

Crivellari, S., Chiessi, C. M., Kuhnert, H., Häggi, C., Portilho-Ramos, R. D., Zeng, J. Y., Zhang, Y., Schefuss, E., Mollenhauer, G., Hefter, J., Alexandre, F., Sampaio, G., and Mulitza, S.: Increased Amazon freshwater discharge during late Heinrich Stadial 1, Quaternary Science Reviews, 181, 144-155, 10.1016/j.quascirev.2017.12.005, 2018.

Curry, W. B. and Oppo, D. W.: Glacial water mass geometry and the distribution of δ13C of ΣCO2 in the western Atlantic Ocean, Paleoceanography, 20, 2005.

Davtian, N. and Bard, E.: A new view on abrupt climate changes and the bipolar seesaw based on paleotemperatures from Iberian Margin sediments, Proceedings of the National Academy of Sciences, 120, e2209558120, 2023.

de Villiers, S., Greaves, M., and Elderfield, H.: An intensity ratio calibration method for the accurate determination of Mg/Ca and Sr/Ca of marine carbonates by ICP-AES, Geochemistry Geophysics Geosystems, 3, 10.1029/2001gc000169, 2002.

Dickson, B., Yashayaev, I., Meincke, J., Turrell, B., Dye, S., and Holfort, J.: Rapid freshening of the deep North Atlantic Ocean over the past four decades, Nature, 416, 832-837, 2002.

Dokken, T. M. and Jansen, E.: Rapid changes in the mechanism of ocean convection during the last glacial period, Nature, 401, 458-461, 10.1038/46753, 1999.

Doughty, A. M., Kaplan, M. R., Peltier, C., and Barker, S.: A maximum in global glacier extent during MIS 4, Quaternary Science Reviews, 261, 106948, 2021.

El Bani Altuna, N., Ezat, M., Greaves, M., and Rasmussen, T. L.: Millennial-scale changes in bottom water temperature and water mass exchange through the Fram Strait 79° N, 63-13 ka, Paleoceanography and Paleoclimatology, 36, e2020PA004061, 2021.

El Bani Altuna, N., Ezat, M. M., Smik, L., Muschitiello, F., Belt, S. T., Knies, J., and Rasmussen, T. L.: Sea ice-ocean coupling during Heinrich Stadials in the Atlantic-Arctic gateway, Scientific Reports, 14, 10.1038/s41598-024-51532-7, 2024.

Elderfield, H., Yu, J., Anand, P., Kiefer, T., and Nyland, B.: Calibrations for benthic foraminiferal Mg/Ca paleothermometry and the carbonate ion hypothesis, Earth and Planetary Science Letters, 250, 633-649, 10.1016/j.epsl.2006.07.041, 2006.

Elderfield, H., Ferretti, P., Greaves, M., Crowhurst, S., McCave, I. N., Hodell, D., and Piotrowski, A. M.: Evolution of ocean temperature and ice volume through the mid-Pleistocene climate transition, Science, 337, 704-709, 10.1126/science.1221294, 2012.

Elderfield, H., Greaves, M., Barker, S., Hall, I. R., Tripati, A., Ferretti, P., Crowhurst, S., Booth, L., and Daunt, C.: A record of bottom water temperature and seawater δ18O for the Southern Ocean over the past 440 kyr based on Mg/Ca of benthic foraminiferal Uvigerina spp, Quaternary Science Reviews, 29, 160-169, 2010.

Evans, H. K., Hall, I. R., Bianchi, G. G., and Oppo, D.: Intermediate water links to Deep Western Boundary Current variability in the subtropical NW Atlantic during marine isotope stages 5 and 4, Paleoceanography, 22, 2007.

Ezat, M. M., Rasmussen, T. L., and Groeneveld, J.: Persistent intermediate water warming during cold stadials in the southeastern Nordic seas during the past 65 k.y, Geology, 42, 663-666, 10.1130/g35579.1, 2014.

https://doi.org/10.5194/egusphere-2026-3334
Preprint. Discussion started: 22 June 2026

745 Farmer, J. R., Keller, K. J., Poirier, R. K., Dwyer, G. S., Schaller, M. F., Coxall, H. K., O'Regan, M., and Cronin, T. M.: A 600 kyr reconstruction of deep Arctic seawater δ 18 O from benthic foraminiferal δ 18 O and ostracode Mg/Ca paleothermometry, Climate of the Past, 19, 555-578, 2023.
Galbraith, E. and de Lavergne, C.: Response of a comprehensive climate model to a broad range of external forcings: relevance for deep ocean ventilation and the development of late Cenozoic ice ages, Climate Dynamics, 52, 653-679,
750 10.1007/s00382-018-4157-8, 2019.
Galbraith, E. D. and Skinner, L. C.: The Biological Pump During the Last Glacial Maximum, Ann Rev Mar Sci, 12, 559-586, 10.1146/annurev-marine-010419-010906, 2020.
Galbraith, E. D., Merlis, T. M., and Palter, J. B.: Destabilization of glacial climate by the radiative impact of Atlantic Meridional Overturning Circulation disruptions, Geophysical Research Letters, 43, 8214-8221, 10.1002/2016gl069846,
755 2016.
Ganopolski, A. and Rahmstorf, S.: Rapid changes of glacial climate simulated in a coupled climate model, Nature, 409, 153-158, 10.1038/35051500, 2001.
Garcia, H. E., Weathers, K. W., Paver, C. R., Smolyar, I. V., Boyer, T. P., Locarnini, R. A., Zweng, M. M., Mishonov, A. V., Baranova, O. K., and Seidov, D.: World Ocean Atlas 2018, volume 3: Dissolved oxygen, apparent oxygen utilization,
760 and dissolved oxygen saturation, 2019.
Garcia-Ibanez, M. I., Pardo, P. C., Carracedo, L. I., Mercier, H., Lherminier, P., Rios, A. F., and Perez, F. F.: Structure, transports and transformations of the water masses in the Atlantic Subpolar Gyre, Progress in Oceanography, 135, 18-36, 2015.
Gherardi, J. M., Labeyrie, L., McManus, J. F., Francois, R., Skinner, L. C., and Cortijo, E.: Evidence from the Northeastern
765 Atlantic basin for variability in the rate of the meridional overturning circulation through the last deglaciation, Earth and Planetary Science Letters, 240, 710-723, 10.1016/j.epsl.2005.09.061, 2005.
Gottschalk, J., Skinner, L. C., Misra, S., Waelbroeck, C., Menviel, L., and Timmermann, A.: Abrupt changes in the southern extent of North Atlantic Deep Water during Dansgaard-Oeschger events, Nature Geoscience, 8, 950-U986, 10.1038/ngeo2558, 2015.
770 Gottschalk, J., Battaglia, G., Fischer, H., Frölicher, T. L., Jaccard, S. L., Jeltsch-Thömmes, A., Joos, F., Köhler, P., Meissner, K. J., Menviel, L., Nehrbass-Ahles, C., Schmitt, J., Schmittner, A., Skinner, L. C., and Stocker, T. F.: Mechanisms of millennial-scale atmospheric CO₂ change in numerical model simulations, Quaternary Science Reviews, 220, 30-74, 10.1016/j.quascirev.2019.05.013, 2019.
Govin, A., Michel, E., Labeyrie, L., Waelbroeck, C., Dewilde, F., and Jansen, E.: Evidence for northward expansion of
775 Antarctic Bottom Water mass in the Southern Ocean during the last glacial inception, Paleoceanography, 24, 10.1029/2008pa001603, 2009.
Gowan, E. J., Zhang, X., Khosravi, S., Rovere, A., Stocchi, P., Hughes, A. L. C., Gyllencreutz, R., Mangerud, J., Svendsen, J. I., and Lohmann, G.: A new global ice sheet reconstruction for the past 80000 years, Nature Communications, 12, 10.1038/s41467-021-21469-w, 2021.
780 Greaves, M., Barker, S., Daunt, C., and Elderfield, H.: Accuracy, standardization, and interlaboratory calibration standards for foraminiferal Mg/Ca thermometry, Geochemistry Geophysics Geosystems, 6, 10.1029/2004gc000790, 2005.
Guihou, A., Pichat, S., Nave, S., Govin, A., Labeyrie, L., Michel, E., and Waelbroeck, C.: Late slowdown of the Atlantic meridional overturning circulation during the last glacial inception: new constraints from sedimentary (231Pa/230Th), Earth and Planetary Science Letters, 289, 520-529, 2010.
785 Guo, Q. M., Li, B. H., Voelker, A. H. L., and Kim, J. K.: Mediterranean Outflow Water dynamics across the middle Pleistocene transition based on a 1.3 million-year benthic foraminiferal record off the Portuguese margin, Quaternary Science Reviews, 247, 10.1016/j.quascirev.2020.106567, 2020.
Hall, I. R. and McCave, I. N.: Palaeocurrent reconstruction, sediment and thorium focussing on the Iberian margin over the last 140 ka, Earth and Planetary Science Letters, 178, 151-164, 2000.
790 Hasenfratz, A. P., Martínez-García, A., Jaccard, S. L., Vance, D., Wälle, M., Greaves, M., and Haug, G. H.: Determination of the Mg/Mn ratio in foraminiferal coatings: An approach to correct Mg/Ca temperatures for Mn-rich contaminant phases, Earth and Planetary Science Letters, 457, 335-347, 10.1016/j.epsl.2016.10.004, 2017.
Haslett, J. and Parnell, A.: A simple monotone process with application to radiocarbon-dated depth chronologies, Journal of the Royal Statistical Society Series C: Applied Statistics, 57, 399-418, 2008.

https://doi.org/10.5194/egusphere-2026-3334
Preprint. Discussion started: 22 June 2026

He, C., Liu, Z., Zhu, J., Zhang, J., Gu, S., Otto-Bliesner, B. L., Brady, E., Zhu, C., Jin, Y., and Sun, J.: North Atlantic subsurface temperature response controlled by effective freshwater input in "Heinrich" events, Earth and Planetary Science Letters, 539, 116247, 2020.

Henry, L. G., McManus, J. F., Curry, W. B., Roberts, N. L., Piotrowski, A. M., and Keigwin, L. D.: North Atlantic ocean circulation and abrupt climate change during the last glaciation, Science, 353, 470-474, 10.1126/science.aaf5529, 2016.

Hodell, D., Crowhurst, S., Skinner, L., Tzedakis, P. C., Margari, V., Channell, J. E. T., Kamenov, G., Maclachlan, S., and Rothwell, G.: Response of Iberian Margin sediments to orbital and suborbital forcing over the past 420 ka, Paleoceanography, 28, 10.1002/palo.20017, 2013.

Hodell, D., Lourens, L., Crowhurst, S., Konijnendijk, T., Tjallingii, R., Jiménez-Espejo, F. J., Skinner, L., Tzedakis, P. C., and Shackleton Site Project, M.: A reference time scale for Site U1385 (Shackleton Site) on the SW Iberian Margin, Global and Planetary Change, 133, 49-64, 10.1016/j.gloplacha.2015.07.002, 2015.

Hodell, D. A., Elderfield, H., Greaves, M., and Party, t. J. S.: JC089 Cruise Report- IODP Site Survey of the Shackleton Sites, SW Iberian Margin, British Ocean Data Centre, 2014.

Hodell, D. A., Crowhurst, S. J., Lourens, L., Margari, V., Nicolson, J., Rolfe, J. E., Skinner, L. C., Thomas, N. C., Tzedakis, P. C., Mleneck-Vautravers, M. J., and Wolff, E. W.: A 1.5-million-year record of orbital and millennial climate variability in the North Atlantic, Climate of the Past, 19, 607-636, 10.5194/cp-19-607-2023, 2023.

Hodell, D. A., Nicholl, J. A., Bontognali, T. R. R., Danino, S., Dorador, J., Dowdeswell, J. A., Einsle, J., Kuhlmann, H., Martrat, B., Mleneck-Vautravers, M. J., Rodríguez-Tovar, F. J., and Röhl, U.: Anatomy of Heinrich Layer 1 and its role in the last deglaciation, Paleoceanography, 32, 284-303, 10.1002/2016pa003028, 2017.

Hoff, U., Rasmussen, T. L., Stein, R., Ezat, M. M., and Fahl, K.: Sea ice and millennial-scale climate variability in the Nordic seas 90 kyr ago to present, Nature Communications, 7, 10.1038/ncomms12247, 2016.

Holloway, M. D., Sime, L. C., Singarayer, J. S., Tindall, J. C., and Valdes, P. J.: Reconstructing paleosalinity from δ18O: coupled model simulations of the Last Glacial Maximum, Last Interglacial and Late Holocene, Quaternary Science Reviews, 131, 350-364, 2016.

Hoogakker, B. A. A., Elderfield, H., Schmiedl, G., McCave, I. N., and Rickaby, R. E. M.: Glacial-interglacial changes in bottom-water oxygen content on the Portuguese margin, Nature Geoscience, 8, 40-43, 10.1038/ngeo2317, 2015.

Howe, J. N., Piotrowski, A. M., Noble, T. L., Mulitza, S., Chiessi, C. M., and Bayon, G.: North Atlantic deep water production during the Last Glacial Maximum, Nature communications, 7, 11765, 2016.

Huang, K.-F., Oppo, D. W., and Curry, W. B.: Decreased influence of Antarctic intermediate water in the tropical Atlantic during North Atlantic cold events, Earth and Planetary Science Letters, 389, 200-208, 2014.

Hughes, P. D., Gibbard, P. L., and Ehlers, J.: Timing of glaciation during the last glacial cycle: evaluating the concept of a global 'Last Glacial Maximum'(LGM), Earth-Science Reviews, 125, 171-198, 2013.

Ivanovic, R., Gregoire, L., Burke, A., Wickert, A. D., Valdes, P., Ng, H. C., Robinson, L., McManus, J., Mitrovica, J., and Lee, L.: Acceleration of northern ice sheet melt induces AMOC slowdown and northern cooling in simulations of the early last deglaciation, Paleoceanography and Paleoclimatology, 33, 807-824, 2018.

Jena, P. S., Chiessi, C. M., Beese, I., Butzin, M., Dias, B. B., Campos, M. d. C., Lohmann, G., and Mulitza, S.: Centennial-scale intensifications of the Atlantic Meridional Overturning Circulation during Heinrich Stadial 1, Nature Communications, 10.1038/s41467-026-73364-x, 2026.

Jenkins, W., Smethie Jr, W., Boyle, E., and Cutter, G.: Water mass analysis for the US GEOTRACES (GA03) North Atlantic sections, Deep Sea Research Part II: Topical Studies in Oceanography, 116, 6-20, 2015.

Jochumsen, K., Köllner, M., Quadfasel, D., Dye, S., Rudels, B., and Valdimarsson, H.: On the origin and propagation of D enmark S trait overflow water anomalies in the I rminger B asin, Journal of Geophysical Research: Oceans, 120, 1841-1855, 2015.

Johnson, G. C.: Quantifying Antarctic Bottom Water and North Atlantic Deep Water volumes, Journal of Geophysical Research-Oceans, 113, 10.1029/2007jc004477, 2008.

Jouzel, J., Masson-Delmotte, V., Cattani, O., Dreyfus, G., Falourd, S., Hoffmann, G., Minster, B., Nouet, J., Barnola, J. M., Chappellaz, J., Fischer, H., Gallet, J. C., Johnsen, S., Leuenberger, M., Loulergue, L., Luethi, D., Oerter, H., Parrenin, F., Raisbeck, G., Raynaud, D., Schilt, A., Schwander, J., Selmo, E., Souchez, R., Spahni, R., Stauffer, B., Steffensen, J. P., Stenni, B., Stocker, T. F., Tison, J. L., Werner, M., and Wolff, E. W.: Orbital and millennial Antarctic climate variability over the past 800,000 years, Science, 317, 793-796, 10.1126/science.1141038, 2007.

https://doi.org/10.5194/egusphere-2026-3334
Preprint. Discussion started: 22 June 2026

Kageyama, M., Merkel, U., Otto-Bliesner, B., Prange, M., Abe-Ouchi, A., Lohmann, G., Ohgaito, R., Roche, D. M., Singarayer, J., Swingedouw, D., and Zhang, X.: Climatic impacts of fresh water hosing under Last Glacial Maximum conditions: a multi-model study, Climate of the Past, 9, 935-953, 10.5194/cp-9-935-2013, 2013.

Kageyama, M., Harrison, S. P., Kapsch, M. L., Lofverstrom, M., Lora, J. M., Mikolajewicz, U., Sherriff-Tadano, S., Vadsaria, T., Abe-Ouchi, A., Bouttes, N., Chandan, D., Gregoire, L. J., Ivanovic, R. F., Izumi, K., LeGrande, A. N., Lhardy, F., Lohmann, G., Morozova, P. A., Ohgaito, R., Paul, A., Peltier, W. R., Poulsen, C. J., Quiquet, A., Roche, D. M., Shi, X. X., Tierney, J. E., Valdes, P. J., Volodin, E., and Zhu, J.: The PMIP4 Last Glacial Maximum experiments: preliminary results and comparison with the PMIP3 simulations, Climate of the Past, 17, 1065-1089, 10.5194/cp-17-1065-2021, 2021.

Klockmann, M., Mikolajewicz, U., and Marotzke, J.: The effect of greenhouse gas concentrations and ice sheets on the glacial AMOC in a coupled climate model, Clim. Past, 12, 1829–1846, 2016.

Knorr, G., Barker, S., Zhang, X., Lohmann, G., Gong, X., Gierz, P., Stepanek, C., and Stap, L. B.: A salty deep ocean as a prerequisite for glacial termination, Nature Geoscience, 14, 930-+, 10.1038/s41561-021-00857-3, 2021.

Lacerra, M., Lund, D., Yu, J., and Schmittner, A.: Carbon storage in the mid-depth Atlantic during millennial-scale climate events, Paleoceanography, 32, 780-795, 10.1002/2016pa003081, 2017.

Leal, A. L., Anderson, R. F., Bausch, A., Fleisher, M. Q., Singh, S. K., Lao, Y., Chinni, V., and Francois, R.: 231Pa/230Th ratios in the Atlantic and Indian Oceans and their implications for the application of the ratios as an ocean circulation proxy, Quaternary Science Reviews, 363, 109448, 2025.

Lerner, P., Marchal, O., Lam, P. J., Gardner, W., Richardson, M. J., and Mishonov, A.: A model study of the relative influences of scavenging and circulation on 230Th and 231Pa in the western North Atlantic, Deep Sea Research Part I: Oceanographic Research Papers, 155, 103159, 2020.

Lippold, J., Gutjahr, M., Blaser, P., Christner, E., de Carvalho Ferreira, M. L., Mulitza, S., Christl, M., Wombacher, F., Böhm, E., and Antz, B.: Deep water provenance and dynamics of the (de) glacial Atlantic meridional overturning circulation, Earth and Planetary Science Letters, 445, 68-78, 2016.

Liu, M. and Tanhua, T.: Water masses in the Atlantic Ocean: characteristics and distributions, Ocean Science, 17, 463-486, 2021.

Liu, Z., Otto-Bliesner, B. L., He, F., Brady, E. C., Tomas, R., Clark, P. U., Carlson, A. E., Lynch-Stieglitz, J., Curry, W., Brook, E., Erickson, D., Jacob, R., Kutzbach, J., and Cheng, J.: Transient Simulation of Last Deglaciation with a New Mechanism for Bolling-Allerod Warming, Science, 325, 310-314, 10.1126/science.1171041, 2009.

Locarnini, R. A., Mishonov, A. V., Baranova, O. K., Reagan, J. R., Boyer, T. P., Seidov, D., Wang, Z., Garcia, H. E., Bouchard, C., and Cross, S. L.: World ocean atlas 2023, volume 1: Temperature, 2024.

Lynch-Stieglitz, J.: The Atlantic meridional overturning circulation and abrupt climate change, Annual review of marine science, 9, 83-104, 2017.

Marcott, S. A., Clark, P. U., Padman, L., Klinkhammer, G. P., Springer, S. R., Liu, Z., Otto-Bliesner, B. L., Carlson, A. E., Ungerer, A., and Padman, J.: Ice-shelf collapse from subsurface warming as a trigger for Heinrich events, Proceedings of the National Academy of Sciences, 108, 13415-13419, 2011.

Margari, V., Skinner, L. C., Menviel, L., Capron, E., Rhodes, R. H., Mleneck-Vautravers, M. J., Ezat, M. M., Martrat, B., Grimalt, J. O., Hodell, D. A., and Tzedakis, P. C.: Fast and slow components of interstadial warming in the North Atlantic during the last glacial, Communications Earth & Environment, 1, 10.1038/s43247-020-0006-x, 2020.

Martrat, B., Grimalt, J. O., Shackleton, N. J., de Abreu, L., Hutterli, M. A., and Stocker, T. F.: Four climate cycles of recurring deep and surface water destabilizations on the Iberian margin, Science, 317, 502-507, 10.1126/science.1139994, 2007.

Mawbey, E. M., Hendry, K. R., Greaves, M. J., Hillenbrand, C.-D., Kuhn, G., Spencer-Jones, C. L., McClymont, E. L., Vadman, K. J., Shevenell, A. E., and Jernas, P. E.: Mg/Ca-Temperature Calibration of Polar Benthic foraminifera species for reconstruction of bottom water temperatures on the Antarctic shelf, Geochimica et Cosmochimica Acta, 283, 54-66, 2020.

Mawbey, E. M., Smith, J. A., Hillenbrand, C.-D., Hendry, K. R., McClymont, E. L., Greaves, M. J., Klages, J. P., Kuhn, G., Radionovskaya, S., and Spencer-Jones, C. L.: Ocean heat forced West Antarctic Ice Sheet retreat after the Last Glacial Maximum, Nature Communications, 2026.

McCave, I. and Andrews, J.: Distinguishing current effects in sediments delivered to the ocean by ice. II. Glacial to Holocene changes in high latitude North Atlantic upper ocean flows, Quaternary Science Reviews, 223, 105902, 2019a.

https://doi.org/10.5194/egusphere-2026-3334
Preprint. Discussion started: 22 June 2026

McCave, I., Manighetti, B., and Robinson, S.: Sortable silt and fine sediment size/composition slicing: parameters for palaeocurrent speed and palaeoceanography, Paleoceanography, 10, 593-610, 1995.
McCave, I. N. and Andrews, J. T.: Distinguishing current effects in sediments delivered to the ocean by ice. I. Principles, methods and examples, Quaternary Science Reviews, 212, 92-107, 10.1016/j.quascirev.2019.03.031, 2019b.
McCave, I. N. and Hall, I. R.: Size sorting in marine muds: Processes, pitfalls, and prospects for paleoflow-speed proxies, Geochemistry Geophysics Geosystems, 7, 10.1029/2006gc001284, 2006.
McManus, J. F., Francois, R., Gherardi, J.-M., Keigwin, L. D., and Brown-Leger, S.: Collapse and rapid resumption of Atlantic meridional circulation linked to deglacial climate changes, nature, 428, 834-837, 2004.
McManus, J. F., Bond, G. C., Broecker, W. S., Johnsen, S., Labeyrie, L., and Higgins, S.: High-resolution climate records from the North Atlantic during the last interglacial, Nature, 371, 326-329, 1994.
Menking, J. A., Shackleton, S. A., Bauska, T. K., Buffen, A. M., Brook, E. J., Barker, S., Severinghaus, J. P., Dyonisius, M. N., and Petrenko, V. V.: Multiple carbon cycle mechanisms associated with the glaciation of Marine Isotope Stage 4, Nat Commun, 13, 5443, 10.1038/s41467-022-33166-3, 2022.
Menviel, L., Timmermann, A., Mouchet, A., and Timm, O.: Meridional reorganizations of marine and terrestrial productivity during Heinrich events, Paleoceanography, 23, 10.1029/2007pa001445, 2008.
Menviel, L., Yu, J., Joos, F., Mouchet, A., Meissner, K., and England, M. H.: Poorly ventilated deep ocean at the Last Glacial Maximum inferred from carbon isotopes: A data-model comparison study, Paleoceanography, 32, 2-17, 2017.
Menviel, L. C., Spence, P., Skinner, L. C., Tachikawa, K., Friedrich, T., Missiaen, L., and Yu, J.: Enhanced Mid-depth Southward Transport in the Northeast Atlantic at the Last Glacial Maximum Despite a Weaker AMOC, Paleoceanography and Paleoclimatology, 35, 10.1029/2019pa003793, 2020.
Mignot, J., Ganopolski, A., and Levermann, A.: Atlantic subsurface temperatures: Response to a shutdown of the overturning circulation and consequences for its recovery, Journal of Climate, 20, 4884-4898, 10.1175/jcli4280.1, 2007.
Muglia, J. and Schmittner, A.: Glacial Atlantic overturning increased by wind stress in climate models, Geophysical Research Letters, 42, 9862-9869, 10.1002/2015gl064583, 2015.
Ng, H. C., Robinson, L. F., McManus, J. F., Mohamed, K. J., Jacobel, A. W., Ivanovic, R. F., Gregoire, L. J., and Chen, T.: Coherent deglacial changes in western Atlantic Ocean circulation, Nature communications, 9, 2947, 2018.
NGRIP Project Members: High-resolution record of Northern Hemisphere climate extending into the last interglacial period, Nature, 431, 147-151, 10.1038/nature02805, 2004.
Oliver, K. I., Hoogakker, B. A., Crowhurst, S., Henderson, G., Rickaby, R. E., Edwards, N., and Elderfield, H.: A synthesis of marine sediment core δ 13 C data over the last 150 000 years, Climate of the Past, 6, 645-673, 2010.
Orsi, A. H., Johnson, G. C., and Bullister, J. L.: Circulation, mixing, and production of Antarctic Bottom Water, Progress in Oceanography, 43, 55-109, 10.1016/s0079-6611(99)00004-x, 1999.
Otto-Bliesner, B. L., Hewitt, C. D., Marchitto, T. M., Brady, E., Abe-Ouchi, A., Crucifix, M., Murakami, S., and Weber, S. L.: Last Glacial Maximum ocean thermohaline circulation: PMIP2 model intercomparisons and data constraints, Geophysical Research Letters, 34, 10.1029/2007gl029475, 2007.
Parnell, A. C., Haslett, J., Allen, J. R., Buck, C. E., and Huntley, B.: A flexible approach to assessing synchroneity of past events using Bayesian reconstructions of sedimentation history, Quaternary Science Reviews, 27, 1872-1885, 2008.
Peck, V. L., Hall, I. R., Zahn, R., Grousset, F., Hemming, S., and Scourse, J.: The relationship of Heinrich events and their European precursors over the past 60 ka BP: a multi-proxy ice-rafted debris provenance study in the North East Atlantic, Quaternary Science Reviews, 26, 862-875, 2007.
Pedro, J. B., Jochum, M., Buizert, C., He, F., Barker, S., and Rasmussen, S. O.: Beyond the bipolar seesaw: Toward a process understanding of interhemispheric coupling, Quaternary Science Reviews, 192, 27-46, 10.1016/j.quascirev.2018.05.005, 2018.
Petit, T., Lozier, M. S., Josey, S. A., and Cunningham, S. A.: Atlantic Deep Water Formation Occurs Primarily in the Iceland Basin and Irminger Sea by Local Buoyancy Forcing, Geophysical Research Letters, 47, 10.1029/2020gl091028, 2020.
Piotrowski, A. M., Goldstein, S. L., Hemming, S. R., and Fairbanks, R. G.: Temporal relationships of carbon cycling and ocean circulation at glacial boundaries, Science, 307, 1933-1938, 10.1126/science.1104883, 2005.
Piotrowski, A. M., Banakar, V. K., Scrivner, A. E., Elderfield, H., Galy, A., and Dennis, A.: Indian Ocean circulation and productivity during the last glacial cycle, Earth and Planetary Science Letters, 285, 179-189, 10.1016/j.epsl.2009.06.007, 2009.

https://doi.org/10.5194/egusphere-2026-3334
Preprint. Discussion started: 22 June 2026

Pöppelmeier, F., Gutjahr, M., Blaser, P., Keigwin, L., and Lippold, J.: Origin of abyssal NW Atlantic water masses since the Last Glacial Maximum, Paleoceanography and Paleoclimatology, 33, 530-543, 2018.

Pöppelmeier, F., Jeltsch-Thömmes, A., Lippold, J., Joos, F., and Stocker, T. F.: Multi-proxy constraints on Atlantic circulation dynamics since the last ice age, Nature Geoscience, 16, 349-+, 10.1038/s41561-023-01140-3, 2023.

Pöppelmeier, F., Gutjahr, M., Blaser, P., Schulz, H., Süfke, F., and Lippold, J.: Stable Atlantic deep water mass sourcing on glacial-interglacial timescales, Geophysical Research Letters, 48, e2021GL092722, 2021.

Pöppelmeier, F., Blaser, P., Gutjahr, M., Jaccard, S. L., Frank, M., Max, L., and Lippold, J.: Northern-sourced water dominated the Atlantic Ocean during the Last Glacial Maximum, Geology, 48, 826-829, 10.1130/g47628.1, 2020.

Radionovskaya, S. and Skinner, L. C.: Changes in bottom-water conditions reconstructed from a depth transect off the Portuguese Coast during MIS 4 and the deglaciation: a micropalaeontological perspective, Quaternary Science Reviews, in review.

Rahmstorf, S.: Ocean circulation and climate during the past 120,000 years, Nature, 419, 207-214, 10.1038/nature01090, 2002.

Rasmussen, S. O., Andersen, K. K., Svensson, A., Steffensen, J. P., Vinther, B. M., Clausen, H. B., Siggaard-Andersen, M. L., Johnsen, S. J., Larsen, L. B., and Dahl-Jensen, D.: A new Greenland ice core chronology for the last glacial termination, Journal of Geophysical Research: Atmospheres, 111, 2006.

Rasmussen, T. L., Oppo, D. W., Thomsen, E., and Lehman, S. J.: Deep sea records from the southeast Labrador Sea: Ocean circulation changes and ice-rafting events during the last 160,000 years, Paleoceanography, 18, 10.1029/2001pa000736, 2003.

Repschlaeger, J., Zhao, N., Rand, D., Lisiecki, L., Muglia, J., Mulitza, S., Schmittner, A., Cartapanis, O., Bauch, H. A., Schiebel, R., and Haug, G. H.: Active North Atlantic deepwater formation during Heinrich Stadial 1, Quaternary Science Reviews, 270, 10.1016/j.quascirev.2021.107145, 2021.

Repschläger, J., Weinelt, M., Andersen, N., Garbe-Schönberg, D., and Schneider, R.: Northern source for Deglacial and Holocene deepwater composition changes in the Eastern North Atlantic Basin, Earth and Planetary Science Letters, 425, 256-267, 10.1016/j.epsl.2015.05.009, 2015.

Rintoul, S. R., Hughes, C. W., and Olbers, D.: The Antarctic circumpolar current system, in: International geophysics, Elsevier, 271-XXXVI, 2001.

Roberts, J., Gottschalk, J., Skinner, L. C., Peck, V. L., Kender, S., Elderfield, H., Waelbroeck, C., Vazquez Riveiros, N., and Hodell, D. A.: Evolution of South Atlantic density and chemical stratification across the last deglaciation, Proc Natl Acad Sci U S A, 113, 514-519, 10.1073/pnas.1511252113, 2016.

Robinson, L. F., Adkins, J. F., Keigwin, L. D., Southon, J., Fernandez, D. P., Wang, S., and Scheirer, D. S.: Radiocarbon variability in the western North Atlantic during the last deglaciation, Science, 310, 1469-1473, 2005.

Rohling, E. J. and Bigg, G. R.: Paleosalinity and δ18O: a critical assessment, Journal of Geophysical Research: Oceans, 103, 1307-1318, 1998.

Rohling, E. J., Grant, K., Hemleben, C., Kucera, M., Roberts, A. P., Schmeltzer, I., Schulz, H., Siccha, M., Siddall, M., and Trommer, G.: New constraints on the timing of sea level fluctuations during early to middle marine isotope stage 3, Paleoceanography, 23, 10.1029/2008pa001617, 2008.

Rohling, E. J., Hibbert, F. D., Williams, F. H., Grant, K. M., Marino, G., Foster, G. L., Hennekam, R., De Lange, G. J., Roberts, A. P., and Yu, J.: Differences between the last two glacial maxima and implications for ice-sheet, δ18O, and sea-level reconstructions, Quaternary Science Reviews, 176, 1-28, 2017.

Rühlemann, C., Mulitza, S., Lohmann, G., Paul, A., Prange, M., and Wefer, G.: Intermediate depth warming in the tropical Atlantic related to weakened thermohaline circulation: Combining paleoclimate data and modeling results for the last deglaciation - art. no. PA1025, Paleoceanography, 19, 10.1029/2003pa000948, 2004.

Sadatzki, H., Dokken, T. M., Berben, S. M. P., Muschitiello, F., Stein, R., Fahl, K., Menviel, L., Timmermann, A., and Jansen, E.: Sea ice variability in the southern Norwegian Sea during glacial Dansgaard-Oeschger climate cycles, Science Advances, 5, 10.1126/sciadv.aau6174, 2019.

Sadekov, A. Y., Bush, F., Kerr, J., Ganeshram, R., and Elderfield, H.: Mg/Ca composition of benthic foraminifera Miliolacea as a new tool of paleoceanography, Paleoceanography, 29, 990-1001, 10.1002/2014pa002654, 2014.

https://doi.org/10.5194/egusphere-2026-3334
Preprint. Discussion started: 22 June 2026

Schönfeld, J. and Zahn, R.: Late Glacial to Holocene history of the Mediterranean Outflow.: Evidence from benthic foraminiferal assemblages and stable isotopes at the Portuguese margin, Palaeogeography Palaeoclimatology Palaeoecology, 159, 85-111, 10.1016/s0031-0182(00)00035-3, 2000.

Seierstad, I. K., Abbott, P. M., Bigler, M., Blunier, T., Bourne, A. J., Brook, E., Buchardt, S. L., Buizert, C., Clausen, H. B., and Cook, E.: Consistently dated records from the Greenland GRIP, GISP2 and NGRIP ice cores for the past 104 ka reveal regional millennial-scale δ18O gradients with possible Heinrich event imprint, Quaternary Science Reviews, 106, 29-46, 2014.

Sessford, E. G., Tisserand, A. A., Risebrobakken, B., Andersson, C., Dokken, T., and Jansen, E.: High-Resolution Benthic Mg/Ca Temperature Record of the Intermediate Water in the Denmark Strait Across D-O Stadial-Interstadial Cycles, Paleoceanography and Paleoclimatology, 33, 1169-1185, 10.1029/2018pa003370, 2018.

Sessford, E. G., Jensen, M. F., Tisserand, A. A., Muschitiello, F., Dokken, T., Nisancioglu, K. H., and Jansen, E.: Consistent fluctuations in intermediate water temperature off the coast of Greenland and Norway during Dansgaard-Oeschger events, Quaternary Science Reviews, 223, 10.1016/j.quascirev.2019.105887, 2019.

Shackleton, N.: Attainment of isotopic equilibrium between ocean water and the benthonic foraminifera genus Uvigerina: isotopic changes in the ocean during the last glacial, 1974.

Shackleton, N. J.: The 100,000-year ice-Age cycle identified and found to lag temperature, carbon dioxide, and orbital eccentricity, Science, 289, 1897-1902, 10.1126/science.289.5486.1897, 2000.

Shackleton, N. J., Hall, M. A., and Vincent, E.: Phase relationships between millennial-scale events 64,000-24,000 years ago, Paleoceanography, 15, 565-569, 10.1029/2000pa000513, 2000.

Shackleton, S., Seltzer, A., Baggenstos, D., and Lisiecki, L. E.: Benthic δ18O records Earth's energy imbalance, Nature Geoscience, 16, 797-802, 2023.

Sherriff-Tadano, S., Abe-Ouchi, A., Yoshimori, M., Oka, A., and Chan, W. L.: Influence of glacial ice sheets on the Atlantic meridional overturning circulation through surface wind change, Climate Dynamics, 50, 2881-2903, 10.1007/s00382-017-3780-0, 2018.

Siddall, M., Rohling, E., Blunier, T., and Spahni, R.: Patterns of millennial variability over the last 500 ka, Climate of the Past, 6, 295-303, 2010.

Siddall, M., Rohling, E. J., Almogi-Labin, A., Hemleben, C., Meischner, D., Schmelzer, I., and Smeed, D.: Sea-level fluctuations during the last glacial cycle, Nature, 423, 853-858, 2003.

Sigman, D. M. and Boyle, E. A.: Glacial/interglacial variations in atmospheric carbon dioxide, Nature, 407, 859-869, 10.1038/35038000, 2000.

Singh, H., Singh, A. D., Tripathi, R., Singh, P., Verma, K., Voelker, A. H. L., and Hodell, D. A.: Centennial-millennial scale ocean-climate variability in the northeastern Atlantic across the last three terminations, Global and Planetary Change, 223, 10.1016/j.gloplacha.2023.104100, 2023.

Skinner, L., Elderfield, H., and Hall, M.: Phasing of millennial climate events and Northeast Atlantic deep-water temperature change since 50 ka BP, Ocean circulation: Mechanisms and impacts—Past and future changes of meridional overturning, 173, 197-208, 2007.

Skinner, L., Menviel, L., Broadfield, L., Gottschalk, J., and Greaves, M.: Southern Ocean convection amplified past Antarctic warming and atmospheric CO₂ rise during Heinrich Stadial 4, Communications Earth & Environment, 1, 10.1038/s43247-020-00024-3, 2020.

Skinner, L. C. and Elderfield, H.: Rapid fluctuations in the deep North Atlantic heat budget during the last glacial period, Paleoceanography, 22, 10.1029/2006pa001338, 2007.

Skinner, L. C. and Shackleton, N. J.: An Atlantic lead over Pacific deep-water change across Termination I: implications for the application of the marine isotope stage stratigraphy, Quaternary Science Reviews, 24, 571-580, 10.1016/j.quascirev.2004.11.008, 2005.

Skinner, L. C., Shackleton, N. J., and Elderfield, H.: Millennial-scale variability of deep-water temperature and δ¹⁸O_{dw} indicating deep-water source variations in the Northeast Atlantic, 0-34 cal. ka BP -: art. no. 1098, Geochemistry Geophysics Geosystems, 4, 10.1029/2003gc000585, 2003.

Skinner, L. C., Freeman, E., Hodell, D., Waelbroeck, C., Riveiros, N. V., and Scrivner, A. E.: Atlantic Ocean Ventilation Changes Across the Last Deglaciation and Their Carbon Cycle Implications, Paleoceanography and Paleoclimatology, 36, 10.1029/2020pa004074, 2021.

https://doi.org/10.5194/egusphere-2026-3334
Preprint. Discussion started: 22 June 2026

Skinner, L. C., Primeau, F., Freeman, E., de la Fuente, M., Goodwin, P. A., Gottschalk, J., Huang, E., McCave, I. N., Noble, T. L., and Scrivner, A. E.: Radiocarbon constraints on the glacial ocean circulation and its impact on atmospheric CO₂, Nature Communications, 8, 10.1038/ncomms16010, 2017.

Stobbe, T. B., Bauch, H. A., Frick, D. A., Yu, J. M., and Gottschalk, J.: Persistent deep-water formation in the Nordic Seas during Marine Isotope Stages 5 and 4 notwithstanding changes in Atlantic overturning, Climate of the Past, 21, 1281-1304, 10.5194/cp-21-1281-2025, 2025.

Thomas, N. C., Bradbury, H. J., and Hodell, D. A.: Changes in North Atlantic deep-water oxygenation across the Middle Pleistocene Transition, Science, 377, 654-659, 10.1126/science.abj7761, 2022.

Thomas, N. C., Ford, H. L., Greaves, M., and Hodell, D. A.: Increased abyssal ocean density stratification across the Middle Pleistocene Transition, EGUsphere, 2025, 1-32, 2025.

Thornalley, D. J., Oppo, D. W., Ortega, P., Robson, J. I., Brierley, C. M., Davis, R., Hall, I. R., Moffa-Sanchez, P., Rose, N. L., and Spooner, P. T.: Anomalously weak Labrador Sea convection and Atlantic overturning during the past 150 years, Nature, 556, 227-230, 2018.

Thornalley, D. J. R., Elderfield, H., and McCave, I. N.: Intermediate and deep water paleoceanography of the northern North Atlantic over the past 21,000 years, Paleoceanography, 25, 10.1029/2009pa001833, 2010.

Thornalley, D. J. R., Elderfield, H., and McCave, I. N.: Reconstructing North Atlantic deglacial surface hydrography and its link to the Atlantic overturning circulation, Global and Planetary Change, 79, 163-175, 10.1016/j.gloplacha.2010.06.003, 2011.

Thornalley, D. J. R., Barker, S., Becker, J., Hall, I. R., and Knorr, G.: Abrupt changes in deep Atlantic circulation during the transition to full glacial conditions, Paleoceanography, 28, 253-262, 10.1002/palo.20025, 2013.

Thornalley, D. J. R., Bauch, H. A., Gebbie, G., Guo, W., Ziegler, M., Bernasconi, S. M., Barker, S., Skinner, L. C., and Yu, J.: A warm and poorly ventilated deep Arctic Mediterranean during the last glacial period, Science, 349, 706-710, 10.1126/science.aaa9554, 2015.

Timmermann, A., Knies, J., Timm, O. E., Abe-Ouchi, A., and Friedrich, T.: Promotion of glacial ice sheet buildup 60–115 kyr BP by precessionally paced Northern Hemispheric meltwater pulses, Paleoceanography, 25, 2010.

Toucanne, S., Rodrigues, T., Menot, G., Soulet, G., Cheron, S., Billy, I., Eynaud, F., Antoine, P., Damste, J. S. S., and Bard, E.: Marine Isotope Stage 4 (71–57 ka) on the Western European margin: Insights to the drainage and dynamics of the Western European Ice Sheet, Global and Planetary Change, 229, 104221, 2023.

Trachsel, M. and Telford, R. J.: All age–depth models are wrong, but are getting better, The Holocene, 27, 860-869, 2017.

Tzedakis, P. C., Drysdale, R. N., Margari, V., Skinner, L. C., Menviel, L., Rhodes, R. H., Taschetto, A. S., Hodell, D. A., Crowhurst, S. J., Hellstrom, J. C., Fallick, A. E., Grimalt, J. O., McManus, J. F., Martrat, B., Mokeddem, Z., Parrenin, F., Regattieri, E., Roe, K., and Zanchetta, G.: Enhanced climate instability in the North Atlantic and southern Europe during the Last Interglacial, Nat Commun, 9, 4235, 10.1038/s41467-018-06683-3, 2018.

Van Aken, H. M.: The hydrography of the mid-latitude northeast Atlantic Ocean: I: The deep water masses, Deep Sea Research Part I: Oceanographic Research Papers, 47, 757-788, 2000.

Vautravers, M. J. and Shackleton, N. J.: Centennial-scale surface hydrology off Portugal during marine isotope stage 3: Insights from planktonic foraminiferal fauna variability, Paleoceanography, 21, 10.1029/2005pa001144, 2006.

Vettoretti, G. and Peltier, W. R.: Interhemispheric air temperature phase relationships in the nonlinear Dansgaard-Oeschger oscillation, Geophysical Research Letters, 42, 1180-1189, 10.1002/2014gl062898, 2015.

Voelker, A. H. L. and de Abreu, L.: A Review of Abrupt Climate Change Events in the Northeastern Atlantic Ocean (Iberian Margin): Latitudinal, Longitudinal, and Vertical Gradients, in: Abrupt Climate Change: Mechanisms, Patterns, and Impacts, edited by: Rashid, H., Polyak, L., and MosleyThompson, E., Geophysical Monograph Book Series, 15-37, 10.1029/2010gm001021, 2011.

Voelker, A. H. L., Lebreiro, S. M., Schönfeld, J., Cacho, I., Erlenkeuser, H., and Abrantes, F.: Mediterranean outflow strengthening during northern hemisphere coolings:: A salt source for the glacial Atlantic?, Earth and Planetary Science Letters, 245, 39-55, 10.1016/j.epsl.2006.03.014, 2006.

Waelbroeck, C., Labeyrie, L., Michel, E., Duplessy, J. C., McManus, J. F., Lambeck, K., Balbon, E., and Labracherie, M.: Sea-level and deep water temperature changes derived from benthic foraminifera isotopic records, Quaternary Science Reviews, 21, 295-305, 10.1016/s0277-3791(01)00101-9, 2002.

https://doi.org/10.5194/egusphere-2026-3334
Preprint. Discussion started: 22 June 2026

Weldeab, S., Arce, A., and Kasten, S.: Mg/Ca-ΔCO3porewater2−–temperature calibration for Globobulimina spp.: A sensitive paleothermometer for deep-sea temperature reconstruction, Earth and Planetary Science Letters, 438, 95-102, 2016a.

Weldeab, S., Friedrich, T., Timmermann, A., and Schneider, R. R.: Strong middepth warming and weak radiocarbon imprints in the equatorial Atlantic during Heinrich 1 and Younger Dryas, Paleoceanography, 31, 1070-1082, 2016b.

Wendt, K. A., Häuselmann, A. D., Fleitmann, D., Berry, A. E., Wang, X. F., Auler, A. S., Cheng, H., and Edwards, R. L.: Three-phased Heinrich Stadial 4 recorded in NE Brazil stalagmites, Earth and Planetary Science Letters, 510, 94-102, 10.1016/j.epsl.2018.12.025, 2019.

Wharton, J. H., Kozikowska, E., Keigwin, L. D., Marchitto, T. M., Maslin, M. A., Ziegler, M., and Thornalley, D. J. R.: Relatively warm deep-water formation persisted in the Last Glacial Maximum, Nature, 10.1038/s41586-025-10012-2, 2026.

Winton, M. and Sarachik, E.: Thermohaline oscillations induced by strong steady salinity forcing of ocean general circulation models, Journal of Physical Oceanography, 23, 1389-1410, 1993.

Wolff, E. W., Chappellaz, J., Blunier, T., Rasmussen, S. O., and Svensson, A.: Millennial-scale variability during the last glacial: The ice core record, Quaternary Science Reviews, 29, 2828-2838, 2010.

Wolff, E. W., Fischer, H., Fundel, F., Ruth, U., Twarloh, B., Littot, G. C., Mulvaney, R., Röthlisberger, R., de Angelis, M., Boutron, C. F., Hansson, M., Jonsell, U., Hutterli, M. A., Lambert, F., Kaufmann, P., Stauffer, B., Stocker, T. F., Steffensen, J. P., Bigler, M., Siggaard-Andersen, M. L., Udisti, R., Becagli, S., Castellano, E., Severi, M., Wagenbach, D., Barbante, C., Gabrielli, P., and Gaspari, V.: Southern Ocean sea-ice extent, productivity and iron flux over the past eight glacial cycles, Nature, 440, 491-496, 10.1038/nature04614, 2006.

Yashayaev, I. and Loder, J. W.: Recurrent replenishment of L abrador S ea W ater and associated decadal-scale variability, Journal of Geophysical Research: Oceans, 121, 8095-8114, 2016.

Yu, J., Menviel, L., Jin, Z. D., Thornalley, D. J. R., Barker, S., Marino, G., Rohling, E. J., Cai, Y., Zhang, F., Wang, X., Dai, Y., Chen, P., and Broecker, W. S.: Sequestration of carbon in the deep Atlantic during the last glaciation, Nature Geoscience, 9, 319-+, 10.1038/ngeo2657, 2016.

Yu, J., Anderson, R. F., Jin, Z. D., Ji, X., Thornalley, D. J. R., Wu, L., Thouveny, N., Cai, Y., Tan, L., Zhang, F., Menviel, L., Tian, J., Xie, X., Rohling, E. J., and McManus, J. F.: Millennial atmospheric CO₂ changes linked to ocean ventilation modes over past 150,000 years, Nature Geoscience, 10.1038/s41561-023-01297-x, 2023.

Yu, J. M. and Elderfield, H.: Mg/Ca in the benthic foraminifera Cibicidoides wuellerstorfi and Cibicidoides mundulus: Temperature versus carbonate ion saturation, Earth and Planetary Science Letters, 276, 129-139, 10.1016/j.epsl.2008.09.015, 2008.

Zahn, R., Sarnthein, M., and Erlenkeuser, H.: Benthic isotope evidence for changes of the Mediterranean outflow during the late Quaternary, Paleoceanography, 2, 543-559, 1987.

Zeng, M., Rashid, H., Lodestro, S., and Gruetzner, J.: Millennial-scale surface water mass changes between the North Atlantic subpolar and subtropical gyre since the last glacial-interglacial cycle, Global and Planetary Change, 253, 104921, 2025.

Zeng, M., Rashid, H., Zhou, Y., McManus, J. F., and Wang, Y.: Dynamics of the subpolar gyre and transition zone of the North Atlantic during the last glacial cycle, Quaternary Science Reviews, 314, 108215, 2023.

Zhang, J. X., Liu, Z. Y., Brady, E. C., Oppo, D. W., Clark, P. U., Jahn, A., Marcott, S. A., and Lindsay, K.: Asynchronous warming and δ18O evolution of deep Atlantic water masses during the last deglaciation, Proceedings of the National Academy of Sciences of the United States of America, 114, 11075-11080, 10.1073/pnas.1704512114, 2017.

Zhang, W. H., Wu, J. Y., Wang, Y., Wang, Y. J., Cheng, H., Kong, X. G., and Duan, F. C.: A detailed East Asian monsoon history surrounding the 'Mystery Interval' derived from three Chinese speleothem records, Quaternary Research, 82, 154-163, 10.1016/j.yqres.2014.01.010, 2014.

Ziemen, F. A., Kapsch, M. L., Klockmann, M., and Mikolajewicz, U.: Heinrich events show two-stage climate response in transient glacial simulations, Climate of the Past, 15, 153-168, 10.5194/cp-15-153-2019, 2019.